Lithos 210–211 (2014) 27–39

Contents lists available at ScienceDirect

Lithos

journal homepage: www.elsevier.com/locate/lithos

Recent plate re-organization at the Azores Triple Junction: Evidence from combined geochemical and geochronological data on Faial, S. Jorge and Terceira volcanic islands

Anthony Hildenbrand [a,b,*], Dominique Weis [c], Pedro Madureira [d,e], Fernando Ornelas Marques [f]

[a] Univ Paris-Sud, Laboratoire GEOPS, UMR8148, Orsay, F-91405, France
[b] CNRS, Orsay, F-91405, France
[c] Pacific Center for Isotope and Geochemical Research, Department of Earth, Ocean and Atmospheric Sciences, University of British Columbia, 2020-2207 Main Mall, Vancouver, BC V6T1Z4, Canada
[d] Estrutura de Missão para a Extensão da Plataforma Continental, R. Costa Pinto, 165, 2770-047, Paço D'Arcos, Portugal
[e] Centro de Geofísica de Évora and Dep. de Geociências da Univ. de Évora, R. Romão Ramalho, 59, 7000-671 Évora, Portugal
[f] Universidade de Lisboa, Lisboa, Portugal

ARTICLE INFO

Article history:
Received 30 March 2014
Accepted 14 September 2014
Available online xxxx

Keywords:
Azores Triple Junction
Geochemistry
K/Ar dating
Melt production
Mantle fertility
Lithospheric deformation

ABSTRACT

The study of volcanism near unstable plate triple junctions (TJs) offers a unique opportunity to investigate the interactions between mantle dynamics and lithospheric deformation in relation to short-term plate reconfiguration. From combined geochronological and geochemical analyses on Terceira, S. Jorge and Faial volcanic islands, we evidence contrasted modes of melt generation near the Azores Triple Junction during the last 1.3 Myr. The oldest lavas (>800 ka) erupted along N150 elongated volcanic systems in S. Jorge and Faial have homogeneous isotopic compositions which partly overlap the compositional field of MORBs from the adjacent Mid-Atlantic Ridge (MAR). In contrast, the younger lavas (<750 ka) erupted along the N110 main structural direction on the three islands are significantly more enriched in LILE and LREE, and have more variable and generally more radiogenic Sr, Pb, Nd and Hf isotopic ratios. Altogether, our data do not support the presence of an active mantle plume under the central Azores. Instead, they suggest that magma generation results from decompression melting of a heterogeneously fertilized mantle (fossil plume?). The higher geochemical heterogeneity of the lavas erupted during the last 750 kyr likely reflects low-degree partial melting promoted by recent reactivation of pre-existing MAR Fracture Zones. We propose that the sub-aerial volcanism over the last 1.3 Myr in the central Azores records a sudden change in the conditions of melt generation, due to a major reconfiguration in regional deformation associated with the recent reorganization of the Eurasia–Nubia plate boundary.

1. Introduction

The evolution of triple junctions (TJs) is a topic of major interest for plate tectonics and geodynamic reconstructions (e.g. Georgen and Lin, 2002; Georgen and Sankar, 2010). In oceanic settings, plate reconfiguration is generally inferred from available magnetic anomaly patterns of the seafloor. However, the mechanisms and the time over which a plate boundary changes its location remain poorly understood, especially in areas where oceanic spreading occurs at very slow rates (e.g. Vogt and Jung, 2004). The study of volcanism occurring close to such TJs offers a unique alternative to overtake these limitations and to constrain the interactions between mantle dynamics, regional deformation, melt production and migration in relation to plate boundary reconfiguration over short geological periods (~1–2 Myr). The Azores volcanic province in the North Atlantic is a target of particular interest for such purpose. The Azores archipelago comprises nine volcanic islands built during the Quaternary (except the easternmost Santa Maria Island) over an oceanic plateau encompassing the present-day TJ between America, Eurasia and Nubia lithospheric plates (Fig. 1). The origin of the volcanism in the Azores has long been attributed to plume–ridge interactions (e.g. Cannat et al., 1999; Lourenço et al., 1998; Luís et al., 1994; Schilling, 1975; Searle, 1980; Vogt and Jung, 2004; White et al., 1976). The Azores plateau, especially, is generally interpreted as a large igneous province (LIP), formed during a plume-derived episode of enhanced melt production centered on the Mid-Atlantic Ridge (MAR) between 20 and 7 Ma ago (e.g. Cannat et al., 1999; Gente et al., 2003). The plateau roughly has a triangular shape, and is delimited in the south by the prominent East Azores Fracture Zone (EAFZ), a presently inactive transform zone interpreted as the fossil eastern branch of the Azores Triple Junction (ATJ). During the last few Myr, the plate boundary between Eurasia and Nubia has jumped to the Terceira Rift (TR), considered an active hyper-slow spreading oceanic rift (e.g. Vogt and Jung, 2004). The

* Corresponding author at: Univ Paris-Sud, Laboratoire GEOPS, UMR8148, Orsay, F-91405, France. Tel.: +33 1 69 15 67 42; fax: +33 1 69 15 48 91.
E-mail address: anthony.hildenbrand@u-psud.fr (A. Hildenbrand).

http://dx.doi.org/10.1016/j.lithos.2014.09.009
0024-4937/

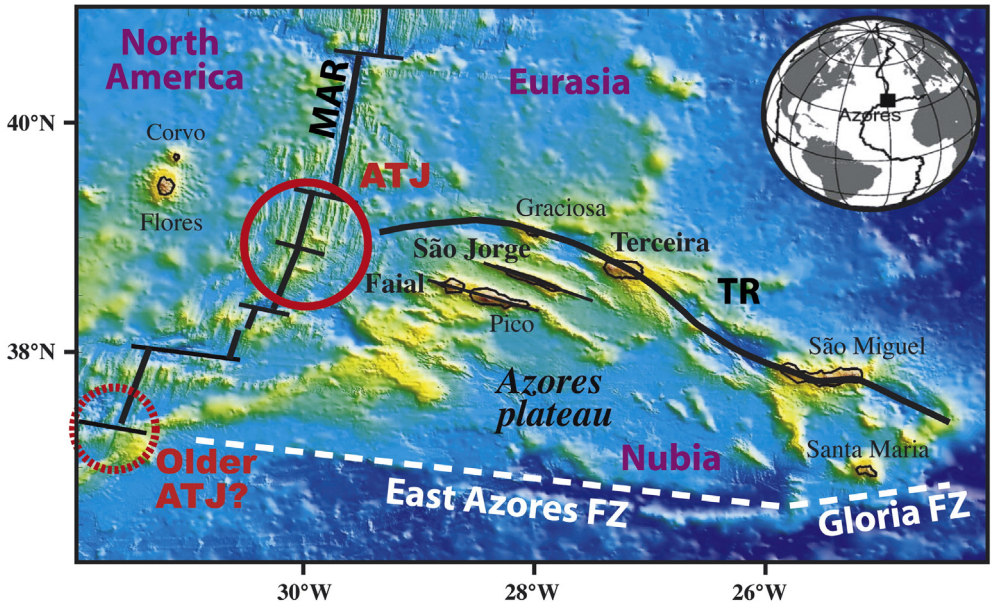

Fig. 1. Main figure: Location of the Azores volcanic archipelago near the triple junction (TJ) between the North American (NA), the Eurasian (EU) and the Nubian (NU) plates. The bold and dotted circles show the location of the present and the older TJ, respectively. Bold black lines show the Mid-Atlantic Ridge (MAR) and the Terceira Rift (TR), and the white line shows the East Azores Fracture Zone. Background bathymetric data from Lourenço et al. (1998). Inset: Location of the Azores region at the Earth surface.

western part of the plate boundary is presently the locus of diffuse deformation distributed along a series of horsts and grabens extending ca. 150 km SW of the TR (e.g., Marques et al., 2013, 2014). Recent volcanism has developed over the plateau, producing numerous elongated submarine and sub-aerial volcanic ridges, with two main directions: N150 and N110–N120 (e.g. Hildenbrand et al., 2008; Lourenço et al., 1998). Recent geochronological studies on the emerged part of some of the ridges have led to significant revisions regarding the timing and the duration of sub-aerial volcanism in the central Azores, and showed that part of the islands have experienced distinct stages of growth most likely controlled by successive episodes of regional deformation (e.g. Hildenbrand et al., 2008, 2012; Silva et al., 2012).

Based on major and trace elements, and isotopic data, several authors pointed out the existence of significant geochemical heterogeneity at the scale of the Azores Archipelago and also at intra-island scale (Beier et al., 2008, 2010, 2012; Davies et al., 1989; Dupré et al., 1982; Elliott et al., 2007; Flower et al., 1976; Haase and Beier, 2003; Madureira et al., 2011; Métrich et al., 2014; Millet et al., 2009; Moreira et al., 1999; Turner et al., 1997; White et al., 1979; Widom et al., 1997). However, very scarce geochronologic data existed at the time of these studies, and as a result, most of the geochemical analyses were performed on lavas of unknown absolute age. It is important to evaluate the link between this heterogeneity and the distinct stages of islands growth since individual events of melt production may have occurred at distinct loci within the mantle, and/or possibly sampled different sources. We here present a new study combining K/Ar dating, major element and high-precision trace element data, and Sr, Nd, Hf and Pb radiogenic analyses on three selected islands from the central Azores: Terceira, S. Jorge and Faial (Fig. 1), which lie in the diffuse part of the Eurasia–Nubia plate boundary. K/Ar dating on fresh-separated groundmass and whole-rock geochemical analyses were systematically carried out on the same samples in order to constrain the evolution of magma geochemistry through time. This allows us to examine temporal and/or geographical variations in the mantle source composition and evaluate the links between TJ reconfiguration and melt production.

2. Sampling location and sample description

Volcanic rocks with no traces of alteration were sampled on the different geological units of the three islands to encompass the main stages of volcanism at the scale of the central Azores (Fig. 2). The location and the characteristics of our samples from S. Jorge and Faial are described in detail elsewhere (Hildenbrand et al., 2008, 2012; Silva et al., 2012). From field relationships, petrographic examination, K/Ar geochronology on separate phases, and whole-rock major and trace element geochemistry, two main eruptive systems have been recognized at S. Jorge: (1) a main N150 volcanic ridge, partly preserved as a ca. 400 m thick lava flow succession in the SE part of the island, which was dated between 1.31 ± 0.02 Ma and 1.21 ± 0.02 Ma (samples AZ05-P, R, U, Z, and AB, Hildenbrand et al., 2008); (2) a more recent N110 volcanic ridge, which experienced episodic short stages of growth over the last 750 kyr (samples AZ05-AC to AZ05-AJ).

Similarly, the evolution of Faial has been controlled by successive short pulses of volcanic construction separated by considerable periods of inactivity (Hildenbrand et al., 2012). The upper part of the older volcanic system is exposed as a ca. 200 m-thick volcanic succession in the eastern end of the island, which has been extensively dated at about 850 ka (samples AZ05-AL to AZ05-AR). Morphologic, structural, paleomagnetic and aerial magnetic data suggest that this old volcanic center had an elongated ridge-like morphology with a main orientation close to the N150 direction (Hildenbrand et al., 2012, 2013). After an apparent volcanic gap of ca. 450 kyr, a small edifice developed on the northeastern corner of the island, between 400 and 350 ka (samples AZ05-AN and AZ05-AP), whereas subsequent activity yielded to the rapid construction of the Central Volcano at about 120 ka (sample AZ05-AO).

New sampling on Terceira Island was carried out on the main central volcanic systems (Calvert et al., 2006; Madureira et al., 2011), i.e. from east to west: (1) the Cinco Picos, (2) the Guilherme-Moniz, and (3) the Santa Bárbara volcanoes. The morphology of Cinco Picos is currently dominated by the largest caldera of the Azores Archipelago (~7 km in diameter) and by a graben (the Lajes Graben) bounded by active normal faults (with a trend N150) in NE Terceira. One of the lowermost accessible lava flows from this succession has been sampled at the shore level (AZ05-C), whereas the topmost lava flow (AZ05-F) has been collected on the upper rim of the Lajes Graben at an altitude of ca. 100 m. A volcanic flow from the same succession has also been sampled within the southern caldera wall (AZ05-K). The Guilherme–Moniz edifice is dominantly composed of differentiated volcanic products, including lava flows and pyroclastic deposits possibly derived from

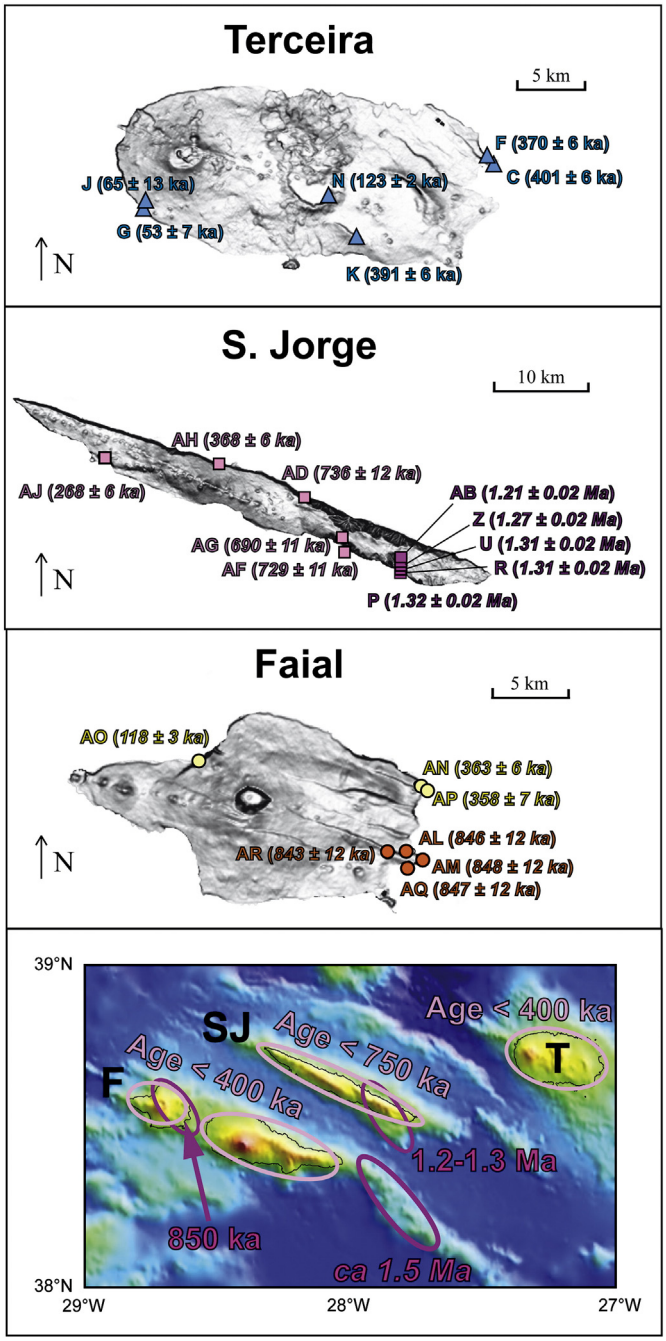

Fig. 2. Upper panels: Location of our samples from Terceira, S. Jorge and Faial (for each sample, prefix "AZ05-" not indicated). Background images are shaded-relief maps built from SRTM topographic data. K/Ar ages are indicated into brackets. New ages measured in this study (Terceira) are shown with normal characters; italic text show previous K/Ar ages obtained on our S. Jorge and Faial samples ((Hildenbrand et al., 2008, 2012; Silva et al., 2012). Lower panel: Synthetic figure showing the age of volcanic construction in the central Azores from unspiked K/Ar data on separated phases (Hildenbrand et al., 2008, 2012; Silva et al., 2012, and this study) and one Ar/Ar age (italic) on the Pico SE submarine volcanic ridge (Beier, 2006). Ellipses show the main elongation of the various volcanic ridges. Background bathymetric data after Lourenço et al. (1998).

multiple vertical caldera collapses (Calvert et al., 2006). A thick trachytic lava flow exposed on the eastern wall of the Gulherme Moniz caldeira was sampled (AZ05-N). The Santa Bárbara volcano is usually thought to be the youngest eruptive system on Terceira (Calvert et al., 2006). Its evolution includes both effusive and explosive eruptions. Part of the volcanic succession has been exposed on the western end of the island by recent coastal erosion. Two lava flows were sampled at the base and top of a western reduced cliff (samples AZ05-G and AZ05-J, respectively). Most of the lavas collected at Terceira Island are subaphyric to slightly porphyric in character, and appear relatively basic in composition. Phenocrysts usually represent less than 10% in volume, and are dominantly composed of olivine and/or clinopyroxene and plagioclase. The microcrystalline groundmass additionally comprises minor oxides. In contrast, the trachyte AZ05-N bears numerous subparallel alkali feldspar elongated crystals.

3. Methods and results

3.1. K/Ar dating

Six new K/Ar determinations on our Terceira samples are presented in this study (Fig. 2), which together with 11 previous ages acquired on S. Jorge (Hildenbrand et al., 2008; Silva et al., 2012), and 15 on Faial (Hildenbrand et al., 2012), amounts to a total of 32 ages acquired with the same protocol of sample preparation and the same analytical procedure on the three islands. After careful petrographic examination of thin-sections, the micro-crystalline groundmass was selected for K/Ar analyses, except for the trachyte from Terceira (sample AZ05-N), from which alkali feldspars have been extracted. In all cases, the rocks were first crushed and sieved at 125–250 μm. Phenocrysts greater than 125 μm in size (olivine, pyroxene, oxides, and plagioclase) were removed with heavy liquids, because they may have crystallized earlier and deeper in the magma chamber. They are thus not representative of the age of eruption at surface, and may carry significant inherited excess argon. Narrow density spans have been achieved to select the freshest part of the groundmass and eliminate the fraction with a lower density, which is potentially affected by minor alteration and secondary zeolitization. Potassium and argon were measured on two separate aliquots of the selected grains, the former by flame emission-spectrophotometry and the latter by mass spectrometry according to the Cassignol–Gillot unspiked technique (details on the analytical procedure in Gillot et al., 2006). Both K and Ar were analyzed at least twice in order to obtain a reproducible value within the range of uncertainties. The used decay constants are from Steiger and Jäger (1977). The results are presented in Table 1, where the uncertainties are quoted at the 1σ level.

The new ages obtained on Terceira range between 401 ± 6 ka and 53 ± 7 ka. The former has been measured on our sample AZ05-C from the base of the old volcanic succession exposed on the NE part of the island. The uppermost lava flow from the same succession (AZ05-F) is dated at 370 ± 6 ka, whereas our sample AZ05-K collected in the middle of the same succession yields a coherent age of 391 ± 6 ka (Table 1 and Fig. 2). These new results are consistent with the ages recently obtained on lava flows sampled at comparable stratigraphic positions and dated between 388 ± 6 ka and 370 ± 2 ka with the $^{40}Ar/^{39}Ar$ step-heating technique (Calvert et al., 2006). The trachyte AZ05-N sampled within the eastern rim of the Guilherm–Moniz caldera in the central part of the island yields an age of 123 ± 2 ka. This age is slightly older than the integrated age of 112 ± 3 ka, but comparable to the isochron age of 118 ± 4 ka determined by furnace step-heating $^{40}Ar/^{39}Ar$ on alkali feldspars from a trachytic body sampled farther west in the upper part of the same succession (Calvert et al., 2006). The two samples from the young volcanic succession exposed on a seacliff on the western end of Terceira yield ages of 61 ± 12 ka and 53 ± 7 ka, which are undistinguishable within the range of uncertainties. These results are consistent with radiocarbon ages obtained on charcoal fragments covered by younger lava flows in the same area (Calvert et al., 2006).

All together, our geochronological data on the three islands show that sub-aerial volcanism in the central Azores has been active during the last 1.3 Myr. S. Jorge and Faial have both experienced "old" subaerial volcanic construction involving the development of N150 ridges, prior to 800 ka. The three islands have been active during the last 750 kyr, and have experienced partly synchronous construction throughout the last 400 kyr (Fig. 2).

Table 1
Results of the new K/Ar dating on our samples from Terceira. The analyses have been performed on fresh-separated groundmass, except for sample AZ05-N (alkali feldspars). The ages are indicated in thousands of years (ka). The uncertainties are reported at the 1σ level.

Sample	Long.	Lat.	Phase	K%	$^{40}Ar^*$ (%)	$^{40}Ar^*$ (10^{12} at/g)	Age (ka)	Unc. (ka)
AZ05-C	−27.0525	38.7334	groundmass	1.258	15.0	0.5263	401	6
					15.5	0.5267	401	6
						mean	**401**	**6**
AZ05-F	−27.0569	38.7346	groundmass	1.182	18.9	0.4609	373	6
					25.3	0.4543	368	5
						mean	**370**	**6**
AZ05-K	−27.1682	38.6746	groundmass	0.992	11.1	0.4097	395	7
					11.9	0.401	387	6
						mean	**391**	**6**
AZ05-N	−27.1945	38.7073	alkali feldspars	4.481	10.8	0.5714	122	2
					11	0.5815	124	2
						mean	**123**	**2**
AZ05-G	−27.3580	38.6931	groundmass	1.136	0.8	0.063	53	7
					0.8	0.063	53	7
						mean	**53**	**7**
AZ05-J	−27.3580	38.6931	groundmass	1.559	0.5	0.0097	60	12
					0.5	0.1156	71	14
						mean	**65**	**13**

3.2. Geochemistry

New whole-rock geochemical analyses have been performed on our samples from the three islands. These include the six Terceira samples dated in the present study (see previous section), and samples from S. Jorge and Faial previously dated by Hildenbrand et al. (2008, 2012) and Silva et al. (2012). A fairly large amount of each sample (about 500 g) was crushed with a hydraulic press and powdered in agate mills to obtain a representative and statistically homogeneous whole-rock powder. For our most porphyritic samples, the separated groundmass extracted for K/Ar dating was also powdered for isotopic analyses.

3.2.1. Major elements

Major elements have been analyzed by XRF and ICP-AES at ALS Chemex (Canada) and Activation Laboratories (Actlabs, Canada), respectively (Table 2). Loss on ignition (LOI) reaches up to 2.2 wt.% (trachyte AZ05-N) but is generally lower than 0.5 wt.% for most of the samples (Table 2), confirming the absence of significant alteration. All the analyzed lavas are alkaline, ranging in composition from basalts to trachytes. The more primitive samples (MgO > 5 wt.%) have relatively high TiO_2, FeO_T and P_2O_5 concentrations compared to typical N-MORB (e.g. Sridhar and Ray, 2003), but similar values compared to other Atlantic OIBs. Most of our samples have Na_2O/K_2O ratios ranging between 1.9 and 3.6. This is similar to values reported for the Azores (excluding S. Miguel) and other Atlantic islands such as Madeira, Saint Helens, Cape Verde and Canary Islands (e.g. Davies et al., 1989; Gurenko et al., 2006; Holm et al., 2006; Wilson, 1989).

Harker-like diagrams show slight but significant variations at both inter and intra-island scales (Fig. 3). Lavas from Terceira are characterized by well-defined and rather narrow trends in most diagrams. In contrast, samples from S. Jorge and Faial exhibit relatively large variations for most oxides at a given MgO. For both islands, compositional differences are observed between lavas older than 800 ka and younger than 750 ka, respectively. This is particularly clear for S. Jorge (Fig. 3), where the youngest samples have higher Na_2O and K_2O, and lower FeO_T and TiO_2 than those from the old volcanic phase (1.3–1.2 Ma). Samples from the young volcanic phases on Faial (<400 ka) also appear to have lower FeO_T and K_2O than the older lavas, whereas no clear difference is observed regarding the other elements. Most of the samples from Faial, however, are more evolved in composition (MgO < 4 wt.%), and exhibit surprisingly high values for Al_2O_3 and CaO (cf. Table 2). Such characteristics are particularly evident for the samples bearing significant amounts of plagioclase phenocrysts/glomerocrysts (e.g. AZ05-AL, AM, AN and AO). Hence the variations observed in these young Faial samples are to be considered with caution, since they partly reflect accumulation processes and/or incorporation of xenocrysts.

3.2.2. Trace elements

Trace elements have been determined for all samples by ICP-MS. Samples from S. Jorge (Hildenbrand et al., 2008) as well as a few samples from Faial were measured previously in Actlabs (Canada). Most of them have been re-analyzed on a Thermofinigan Element 2 at the Pacific Center for Isotopic and Geochemical Research at the University of British Columbia (PCIGR, UBC), in Canada, following the procedure reported in Pretorius et al. (2006) and Carpentier et al. (2013). The results are presented in Table 2. Values obtained on duplicate and replicate measurements on our sample AZ05-AF and on reference material BHVO-2, BCR2 and Kil93 are shown additionally in Supplementary material S1. The results obtained at PCIGR and at Actlabs on several samples from S. Jorge are generally consistent, allowing a meaningful comparison of the few samples not analyzed in both laboratories.

The three islands have overall similar patterns in extended trace element diagrams normalized to primitive mantle (Fig. 4). All the lavas are highly enriched in incompatible elements, especially LILE (e.g., Ba, Rb), LREE (e.g., La, Ce, Nd), and several HFSE (e.g., Nb, Ta). The most evolved lavas (MgO < 4 wt.%) show a positive shift towards higher concentrations for most elements. The trachytic sample from Terceira (AZ05-N) is additionally marked by prominent negative anomalies of Ba, Sr and Eu, most probably reflecting fractionation and removal of alkali feldspars and plagioclase.

All the analyzed lavas are enriched in REE relative to chondrite C1 (McDonough and Sun, 1995). They show enrichment by more than a factor of 100 in light REE (La, Ce, Pr, Nd) and the typical trend observed for alkaline OIB. Ratios between LREE and MREE (e.g. La/Sm) in mafic samples (MgO > 4 wt.%) are significantly higher than those reported for Atlantic N-MORB (e.g. Debaille et al., 2006), but comparable to the values from the adjacent part of the MAR between latitudes 39°N and 39.5°N (Dosso et al., 1999). At the scale of the three islands, the lavas erupted prior to 800 ka and after 750 ka show significant differences. The oldest lavas from both S. Jorge and Faial plot as a linear and relatively narrow trend in the $(La/Yb)_N$ vs. La diagram, whereas the young samples from the three islands show higher values and a greater dispersion (Fig. 5). We note that the highest $(La/Yb)_N$ ratios do not simply correlate with low MgO, and hence rule out a significant artifact due to differentiation processes. Further differences between old and young volcanics are also observed from incompatible element ratios, e.g. on the Zr/Nb vs. Rb/Th diagram, where two main groups can be identified. The oldest

lavas from both S. Jorge and Faial have relatively high Zr/Nb and Rb/Th compared to the young volcanics from the three islands.

3.2.3. Radiogenic isotopes

The Sr–Nd–Pb–Hf isotopic compositions of all our samples have been measured at PCIGR. Full details on the protocol of sample preparation (including repeated leaching), analytical procedures, and data reduction are provided elsewhere (Hanano et al., 2009; Nobre Silva et al., 2009, 2010, 2013; Weis and Frey, 1991, 1996; Weis et al., 2005, 2006, 2007), and summarized in Supplementary file S2. Measurements on BHVO-2 and BCR-2 reference material prepared along with our samples (Table 2) yielded results within the range of values reported in Weis et al. (2005, 2006, 2007) for $^{87}Sr/^{86}Sr$, $^{143}Nd/^{144}Nd$, $^{206}Pb/^{204}Pb$, $^{207}Pb/^{204}Pb$, $^{208}Pb/^{204}Pb$ and $^{176}Hf/^{177}Hf$. Duplicate measurements on distinct aliquots of sample AZ05-AF give consistent results for all isotopic ratios within the range of analytical uncertainties. Replicate measurements on the solution of a few samples also yield reproducible results, with a relative variability less than 100 ppm for all isotopic ratios (Supplementary file S3). The isotopic composition measured on both whole-rock and groundmass for some of our samples is in most cases indistinguishable within the range of uncertainties (Table 3).

The new results obtained on the different samples from the three islands are constrained within the range of values previously measured on central Azores (e.g. Beier et al., 2012; Dupré et al., 1982; Elliott et al., 2007; Halliday et al., 1992; Madureira et al., 2011; Millet et al., 2009; Moreira et al., 1999; Oversby, 1971; Turner et al., 1997; White and Hofmann, 1982; White et al., 1979). The Sr and Nd isotopic compositions define a somewhat linear relationship (Fig. 6), partly overlapping the field of MORB data from the adjacent portion of the MAR (Agranier et al., 2005; Dosso et al., 1999). The three islands overall exhibit a limited range of variations, except the trachyte AZ05-N, which shows a very high $^{87}Sr/^{86}Sr$ ratio (0.705523 ± 0.000009). Lavas from S. Jorge generally have a slightly higher $^{143}Nd/^{144}Nd$ than the other islands for comparable Sr isotopic ratios (except sample AZ05-AH), whereas Faial is shifted towards higher $^{87}Sr/^{86}Sr$ values. All the analyzed samples are characterized by relatively high $^{208}Pb/^{204}Pb$, $^{207}Pb/^{204}Pb$ and $^{206}Pb/^{204}Pb$ values, in agreement with recently published values on the central Azores (e.g. Beier et al., 2008, 2012; Elliott et al., 2007; Madureira et al., 2011; Millet et al., 2009). In $^{208}Pb/^{204}Pb$ vs. $^{206}Pb/^{204}Pb$ and $^{207}Pb/^{204}Pb$ vs. $^{206}Pb/^{204}Pb$ diagrams (Fig. 7), most samples define a linear trend, located below the Northern Hemisphere Reference Line (NHRL, Hart, 1984). The oldest lavas from S. Jorge and Faial (age > 800 ka) exhibit a limited range of compositions partly overlapping the field of local MORBs. The young lavas from the three islands (age < 750 ka) show more heterogeneity, and plot as two main groups: (1) one group comprises all the samples from Terceira and most of the young samples from S. Jorge, which largely overlap with respect to each other; (2) the other group includes the three youngest samples from Faial (samples AZ05-AN, AZ05-AO, and AZ05-APg) and sample AZ05-AH from S. Jorge, which plot above the NHRL with a $^{206}Pb/^{204}Pb$ significantly lower than all the other lavas. These peculiar samples are also characterized by $^{87}Sr/^{86}Sr$ ratios higher than 0.70375 (see Table 3 and Fig. 6).

The Hf isotopic composition of our samples has relatively limited range of values constrained between 0.28296 and 0.28311 (2σ uncertainties included). These are similar to the values reported on the young (<300 ka) island of Pico, but significantly higher than those measured on samples from S. Miguel (Elliott et al., 2007; Snyder et al., 2004). In the Hf–Nd and Hf–Sr isotopic spaces (Fig. 8), our samples from the three islands define linear relationships sub-parallel to the trend defined by MORB data from the adjacent portion of the MAR (Agranier et al., 2005), but slightly shifted towards more radiogenic Sr and Nd ratios. Moreover, the Hf isotopic composition of the lavas does not appear to be correlated with Pb isotope systematics (Fig. 8).

In a plot of the isotopic composition of the samples as a function of their eruption age (Fig. 9), a clear distinction can be made between the samples erupted prior to 800 ka and those after 750 ka. The samples from S. Jorge and Faial N150 volcanic ridges (age > 800 ka) overall have rather homogeneous and weakly radiogenic compositions. In contrast, the lavas erupted over the last 750 kyr along the N110 direction show higher $^{207}Pb/^{204}Pb$ (up to 15.64) and a large range of variations in $^{208}Pb/^{204}Pb$ and $^{206}Pb/^{204}Pb$, from weakly radiogenic to very radiogenic ratios.

4. Discussion

4.1. Source components and mantle heterogeneity

The new isotopic compositions measured in this study are generally less dispersed than previous isotopic data obtained in the central Azores islands (Figs. 6–8). This can be partly explained by the steadiness of the analytical conditions at PCIGR (for a review see Weis et al., 2005, 2006, 2007) and by the peculiar procedure of sample preparation here adopted. Repeated leaching, especially, is particularly important for measuring the pristine composition of volcanic products in such oceanic environments, and to remove eventual in-situ superficial contamination by sea water, or secondary contamination during crushing of the samples, as shown by recent systematic studies (e.g. Hanano et al., 2009; McDonough and Chauvel, 1991; Nobre Silva et al., 2009, 2010; Weis and Frey, 1991, 1996; Weis et al., 2005, 2006, 2007). We note, however, that leaching may not have been sufficient to fully remove contamination by seawater in the case of our sample AZ05-N, which shows an extremely high $^{87}Sr/^{86}Sr$ ratio. This sample also has a very low Sr elementary content (ca. 20 ppm in whole-rock). Therefore, a very small residual contamination by seawater could be sufficient to shift the $^{87}Sr/^{86}Sr$ ratios, without significantly affecting the other isotopic ratios. In contrast, values obtained on all the other samples are mutually consistent, and the high reproducibility amongst the various duplicates and replicates rules out any significant surficial contamination. Similarly, the isotopic ratios obtained on both whole-rock and groundmass for the most porphyric samples from Faial (AZ05-AL, AM, AN and AO) and S. Jorge (AZ05-AB, AZ05-AD) show that the isotopic ratios measured on whole-rock samples are not biased by any eventual incorporation of inherited xenoliths or phenocrysts from earlier magma production events.

The narrow compositional trends observed in the Nd–Sr, Pb–Pb, Hf–Nd and Sr–Pb isotopic spaces in samples from the three islands are here interpreted as reflecting mixing between distinct source components or "end-members." From our new data, three components can be distinguished and compared with end-members previously recognized in the Azores (Figs. 6–8): (1) a weakly radiogenic component dominantly expressed in our oldest samples from both S. Jorge and Faial (Figs. 6–8). It has $^{87}Sr/^{86}Sr$, $^{143}/^{144}Nd$, $^{208}Pb/^{204}Pb$, $^{206}Pb/^{204}Pb$ and $^{176}Hf/^{177}Hf$ ratios close to the average composition of MORBs from the adjacent MAR between latitudes 37°N and 40°N (e.g. Agranier et al., 2005; Dosso et al., 1999), represented by a star in Fig. 7. We note that the $^{207}Pb/^{206}Pb$ isotopic ratios of our oldest samples are significantly lower than the average regional MORB composition, but remain close to the composition of some individual MAR samples. The weakly radiogenic component here inferred thus most likely reflects the involvement of regional upper mantle signature during melt generation. (2) A HIMU-type component is fairly clear from the isotopic composition of most of our samples. It has values similar to the local "end-member" recognized in Terceira and S. Jorge lavas (e.g. Madureira et al., 2011; Millet et al., 2009; Turner et al., 1997), and referred to as "T" in Fig. 7. The nature and the amount of recycled material possibly involved in the HIMU-like component has been extensively discussed in earlier studies (e.g. Madureira et al., 2011; Millet et al., 2009), and is beyond the scope of this paper. We note, however, that $^{87}Sr/^{86}Sr$ ratios measured here and in previous works on the central Azores are somewhat higher than in typical HIMU signatures recognized elsewhere, e.g. in the Cook–Australes chain in the Pacific (Chauvel et al., 1992; Hofmann, 2003; Jackson and Dasgupta, 2008), which suggests possible recycling of both highly altered oceanic crust and sediments by old subduction processes. (3) A third component can be distinguished in the three young samples

Table 2
Whole-rock major and trace element composition of our samples from S. Jorge, Terceira and Faial. For each sample, the eruption age measured by unspiked K/Ar dating on separated phase is indicated: *this study; **data from Hildenbrand et al. (2008); ***data from Silva et al. (2012); ****data from Hildenbrand et al. (2012).

Island	Terceira	Terceira	Terceira	Terceira	Terceira	Terceira	Sao Jorge	Sao Jorge	Sao Jorge	Sao Jorge	Sao Jorge	Sao Jorge
Sample	AZ05-C	AZ05-F	AZ05-G	AZ05-J	AZ05-K	AZ05-N	AZ05-P	AZ05-R	AZ05-U	AZ05-Z	AZ05-AB	AZ05-AD
Long. (W)	27.0525	27.0569	27.358	27.358	27.168	27.1948	27.8662	27.8553	27.8559	27.8571	27.8517	27.9682
Lat. (N)	38.7334	38.7346	38.6931	38.6931	38.6746	38.7073	38.5601	38.547	38.5482	38.5503	38.5479	38.6388
Age ± unc. (ka)	401 ± 6*	370 ± 6*	53 ± 7*	65 ± 13*	391 ± 6*	122 ± 2*	1323 ± 21**	1310 ± 19**	1314 ± 19***	1267 ± 18***	1207 ± 17**	736 ± 12**
Unnormalized major element oxides (wt.%)												
Analytical technique	XRF	XRF	ICP-OES	ICP-OES	XRF	XRF	ICP-OES	ICP-OES	ICP-OES	ICP-OES	ICP-OES	ICP-OES
SiO_2	47.26	47.8	48.21	50.96	47.27	64.09	43.28	47.26	47.28	52.9	48.09	45.63
TiO_2	3.8	4.02	3.7	2.96	4.4	0.59	4.43	3.49	3.43	2.24	2.78	2.94
Al_2O_3	15.27	15.49	16.02	15.83	14.81	13.29	15.62	15.64	15.78	17	20.43	15.36
Fe_2O_3*	13.3	13.46	12.07	11.28	13.77	7.46	14.18	12.23	12.39	9.7	9.76	11.72
MnO	0.2	0.22	0.18	0.2	0.21	0.34	0.18	0.17	0.18	0.17	0.13	0.16
MgO	4.73	4.02	4.58	3.5	4.83	0.7	5.49	4.44	4.34	2.85	3.28	8.98
CaO	9.17	7.98	9.78	7.85	9.17	0.69	9.93	8.42	8.35	6.04	9.98	10.35
Na_2O	3.52	3.81	3.56	4.35	3.45	6.03	2.65	3.52	3.68	5.1	3.31	2.88
K_2O	1.39	1.38	1.22	1.74	1.25	4.43	0.88	1.49	1.63	2.44	1.17	0.87
P_2O_5	0.65	0.76	0.63	0.83	0.86	0.05	0.57	0.74	0.82	0.89	0.53	0.46
LOI	−0.1	0.54	−0.312	−0.31	−0.31	2.16	1.52	2.04	1.52	0.03	0.35	0.26
Total	99.3	99.61	99.65	99.19	99.83	99.82	98.73	99.43	99.4	99.36	99.81	99.64
Trace elements (ppm)												
Lab.	*PCIGR*	*PCIGR*	*PCIGR*	*PCIGR*	*PCIGR*	*PCIGR*	*PCIGR*	*PCIGR*	*PCIGR*	*PCIGR*	*PCIGR*	*PCIGR*
La	34.87	43.98	37.35	51.5	45.31	167.84	28.44	37.19	39.95	60.69	24.55	27.07
Ce	78.7	81.9	80.8	109.1	90.7	321.3	67	85.2	88.3	126	55.7	60.6
Pr	9.98	12.23	10.14	13.27	12.28	36.19	8.78	11.03	11.75	15.6	7.31	7.74
Nd	42.4	51.9	41.8	54.1	51	130.1	37.6	46.4	48.8	63.6	31.4	32.2
Sm	8.72	10.65	8.76	11.2	10.69	24.53	8.52	10.24	10.85	13.05	6.86	6.61
Eu	2.92	3.7	2.92	3.61	3.62	3.53	2.83	3.37	3.61	4.03	2.5	2.25
Gd	9.55	11.29	9.16	11.77	11.29	30.68	8.97	10.84	11.52	13.52	7.49	7.37
Tb	1.42	1.66	1.33	1.72	1.63	4.17	1.32	1.62	1.68	2.03	1.1	1.04
Dy	7.86	8.95	7.16	9.24	8.99	25	7.21	8.75	9.03	11.13	6.01	5.52
Ho	1.33	1.46	1.15	1.51	1.43	4.38	1.17	1.45	1.49	1.81	0.96	0.91
Er	3.72	4.07	3.19	4.19	3.91	13.19	3.19	3.9	4.02	5.14	2.66	2.47
Tm	0.47	0.5	0.4	0.54	0.48	1.83	0.4	0.51	0.51	0.65	0.33	0.32
Yb	3.02	3.18	2.57	3.32	3.05	12.21	2.52	3.14	3.27	4.29	2.17	2.05
Lu	0.42	0.44	0.35	0.47	0.4	1.69	0.34	0.42	0.44	0.57	0.29	0.27
Sc	20.38	19.33	21.38	17.18	24.7	4.17	26.72	23.28	22.22	14.25	15.58	25.7
V	355	296	339	250	349	–	394	276	254	132	199	258
Cr	5	–	57	15	7	–	15	1	–	4	8	250
Co	37	31	36	25	39	1	44	30	29	17	24	51
Ni	20	–	38	9	13	–	34	7	2	4	15	135
Cu	26	5	30	15	20	1	26	24	18	11	18	24
Zn	112	123	110	127	129	312	125	137	136	134	94	102
Ga	21	23	24	26	23	40	24	26	26	28	25	20
Rb	29	29	25	39	28	119	18	30	33	57	25	20
Sr	524	557	684	641	634	23	622	580	599	536	795	688
Y	31.6	37.7	30.7	43.7	41.6	126.3	31.7	41.6	43.5	53	26.1	23.9
Zr	258	262	295	388	258	1630	261	361	375	580	248	224
Nb	52	51.3	55.5	73.1	52.9	284.3	41.7	55.6	57.6	81.8	36.2	35.6
Cs	0.2	0.1	0.1	0.2	0.2	1.7	0.1	0.2	0.2	0.3	0.3	0.2
Ba	393	525	316	431	428	74	243	315	339	510	310	244
Hf	6.6	6.5	6.6	8.7	6	34.5	6.2	8.2	8.6	12	5.6	5.3
Ta	3.39	3.25	3.17	3.93	2.98	14.52	2.58	3.2	3.27	4.49	2.19	2.2
Pb	2.24	2.01	1.58	2.27	1.67	10.77	1.15	1.61	1.64	2.84	1.26	1.47
Th	3.71	3.14	3.46	4.97	2.87	19.7	2.36	3.27	3.26	6.01	2.19	2.5
U	1.09	0.95	1.21	1.69	0.91	6.65	0.88	1.17	1.16	1.86	0.71	0.87

from Faial and our young sample AZ05-AH from S. Jorge. Their position to the left of the NHRL line in the Pb/Pb isotopic spaces points to a significantly lower $^{206}Pb/^{204}Pb$, whereas Figs. 6–8 show a significantly higher $^{87}Sr/^{86}Sr$, and lower $^{143}Nd/^{144}Nd$ and $^{176}Hf/^{177}Hf$ with respect to other lavas. This suggests a source with compositional similarities to the EM-like component previously recognized or suspected in Faial, S. Jorge and Terceira (e.g. Madureira et al., 2011; Millet et al., 2009). The third component may thus represent small amounts of recycled residual lithologies, e.g. delaminated sub-continental lithospheric fragments which, like the HIMU component, have been preferentially incorporated during recent melt generation over the last 750 kyr.

4.2. Geodynamic controls on melt production

The genesis of the volcanism in the Azores has long been attributed either to a plume-like mantle anomaly, which would carry temperature excess (e.g. Bourdon et al., 2005) and volatile-rich material to the upper mantle (Asimow et al., 2004; Beier et al., 2012) or to a hydrated upper mantle source (Bonatti, 1990). Recent data on melt and fluid inclusions trapped in young basaltic scoriae from Pico Island, especially, suggest the presence of a “wet spot” (Métrich et al., 2014). The HIMU and EM-type components recognized here and in some previous studies would reflect the dual signature of the components incorporated in the Azores

Island	Sao Jorge	Sao Jorge	Sao Jorge	Sao Jorge	Faial	Faial	Faial	Faial	Faial	Faial	Faial
Sample	AZ05-AF average	AZ05-AG	AZ05-AH	AZ05-AJ	AZ05-AL	AZ05-AM	AZ05-AN	AZ05-AO	AZ05-AR	AZ05-AQ	AZ05-AP
Long. (W)	27.9213	27.9399	28.0713	28.204	28.6094	28.6073	28.6045	28.75	28.625		28.6015
Lat. (N)	38.5773	38.591	38.6793	38.68162	38.5524	38.5502	38.5963	38.6159	38.5528		38.5946
Age ± unc. (ka)	729 ± 11**	690 ± 11**	368 ± 6**	268 ± 6**	846 ± 12****	848 ± 12****	363 ± 6****	118 ± 3****	843 ± 12****	847 ± 12****	358 ± 7****
Analytical technique	ICP-OES	ICP-OES	ICP-OES	ICP-OES	ICP-OES	ICP-OES	XRF	XRF	ICP-OES	ICP-OES	ICP-OES
SiO_2	45.24	48.26	45.1	47.04	49.14	48.93	46.7	49.77	50.09	49.16	47.62
TiO_2	3.9	3.22	3.97	3.48	2.32	2.46	3.09	2.41	3.02	2.78	3.22
Al_2O_3	16.6	16.45	14.74	16.37	19.44	18.89	19.91	20.93	17	18.42	18.13
Fe_2O_3*	12.6	11.87	12.31	12.18	9.46	9.95	10.14	8.08	11.4	10.54	11.36
MnO	0.18	0.2	0.18	0.17	0.15	0.162	0.14	0.14	0.19	0.17	0.17
MgO	5.6	4.17	8.27	6.04	3.5	3.65	4.09	2.89	3.44	3.41	4.32
CaO	9.33	7.92	9.98	8.84	10.11	9.8	10.54	9.11	7.29	9	9.24
Na_2O	3.59	4.81	2.93	3.81	3.89	3.77	2.85	4.24	4.16	3.85	3.7
K_2O	1.11	1.5	1.54	1.41	1.49	1.56	1.18	1.59	2.28	1.87	1.49
P_2O_5	0.66	1.21	0.67	0.78	0.45	0.48	0.43	0.52	0.65	0.53	0.58
LOI	−0.16	−0.35	−0.52	−0.32	0.254	0.52	0.63	0.05	0.7	0.32	0.22
Total	98.64	99.27	99.17	99.82	100.2	100.2	99.83	99.87	100.2	100.05	100.04
Lab.	*PCIGR*	*PCIGR*	*PCIGR*	*PCIGR*	*Actlab*	*PCIGR*	*PCIGR*	*PCIGR*	*PCIGR*	*Actlab*	*Actlab*
La	37.45	50.19	41.45	41.6	28.5	27.46	30.5	37.74	44.01	32.3	36.1
Ce	82.1	109.4	92.3	90	60.6	60.8	66.2	83.5	89.3	69.7	79
Pr	10.61	14.41	11.44	11.48	7.02	7.43	8.21	10.1	11.24	8.11	9.18
Nd	44.6	61	45.3	47.6	28.6	30.3	32.8	40.5	44.8	33.1	37.4
Sm	9.06	12.9	8.86	9.31	5.94	6.18	6.8	7.81	9.27	7.03	7.75
Eu	3.01	4.24	2.85	3.09	2.29	2.12	2.39	2.77	3.11	2.65	2.93
Gd	9.52	13.59	9.8	9.79	5.85	6.84	7.35	8.42	10.07	6.98	7.36
Tb	1.37	1.98	1.28	1.4	0.95	1.02	1.1	1.22	1.51	1.16	1.23
Dy	7.38	10.45	6.68	7.44	5.51	5.75	5.93	6.67	8.31	6.46	6.7
Ho	1.19	1.71	1.04	1.17	1.04	0.99	0.97	1.08	1.43	1.21	1.23
Er	3.28	4.49	2.87	3.25	2.9	2.84	2.74	3.04	4.07	3.39	3.38
Tm	0.41	0.57	0.35	0.4	0.41	0.38	0.35	0.39	0.54	0.48	0.45
Yb	2.62	3.65	2.3	2.61	2.54	2.49	2.21	2.48	3.51	2.91	2.68
Lu	0.35	0.49	0.31	0.35	0.38	0.34	0.3	0.35	0.49	0.4	0.384
Sc	21.86	16.43	27.08	19.82	16	17.97	22.1	13.39	19.38	18	20
V	308	190	324	271	240	273	257	176	202	256	262
Cr	44	5	277	111	20	29	40	13	5	–	–
Co	39	24	47	38	23	26	29	18	24	23	28
Ni	37	8	130	59	18	21	22	9	4	13	13
Cu	21	11	26	26	24	16	16	13	13	26	23
Zn	114	135	110	121	77	92	92	86	138	82	93
Ga	23	24	22	25	23	23	23	25	23	23	24
Rb	24	33	27	27	30	30	23	35	45	35	24
Sr	792	797	725	740	638	607	765	822	548	575	710
Y	30.7	47.3	27.2	31.1	28.4	26.3	25.3	27.2	37.2	32.9	33.1
Zr	292	375	337	354	206	235	236	286	336	254	260
Nb	55	66	61.8	63.4	35.1	40.5	36.4	49.8	55.1	38.5	41.3
Cs	0.2	0.3	0.2	0.2	0.3	0.2	0.1	0.3	0.3	0.2	0.3
Ba	294	411	320	325	348	351	357	425	499	418	407
Hf	7	8.8	7.6	7.4	4.7	5.2	5.6	6.8	8	5.6	5.9
Ta	3.34	3.66	3.69	3.66	2.72	2.38	2.15	3.05	3.34	3.08	3.28
Pb	1.76	2.2	1.9	1.88	5	2.1	1.94	2.8	2.48	4	–
Th	3.54	3.94	3.75	3.82	2.77	2.87	2.97	4.18	4.44	2.99	3.27
U	1.21	1.42	1.18	1.22	0.67	0.85	0.76	1.31	1.35	0.9	1.14

plume (Turner et al., 1997), whereas primitive helium and neon isotopic compositions have been interpreted as evidence for sampling of a relatively undegassed "reservoir" attributed to the deep mantle (Jean-Baptiste et al., 2009; Madureira et al., 2005; Moreira et al., 2012). However, the location, the size and the dynamics of the inferred plume remain elusive. From seismic tomographic modeling, somewhat contradictory conclusions have been reached. Global tomographic models argue for a low-velocity zone down to 1000 km depth, interpreted as evidence for a deep-seated plume rising from the lower mantle (Montelli et al., 2004, 2006), whereas regional tomographic models (e.g. Pilidou et al., 2005; Silveira et al., 2006) emphasize the presence of a main shallow anomaly (<200 km) under the Azores plateau, possibly rooted at the transition between the lower and upper mantles a few tens of km NE of Terceira (Adam et al., 2013; Yang et al., 2006). From geochemical data, most authors explicitly or implicitly consider "the Azores plume" as an active narrow feature, which would be either centered along the MAR (White et al., 1976), under Terceira (Bourdon et al., 2005), or even under Pico (Beier et al., 2012).

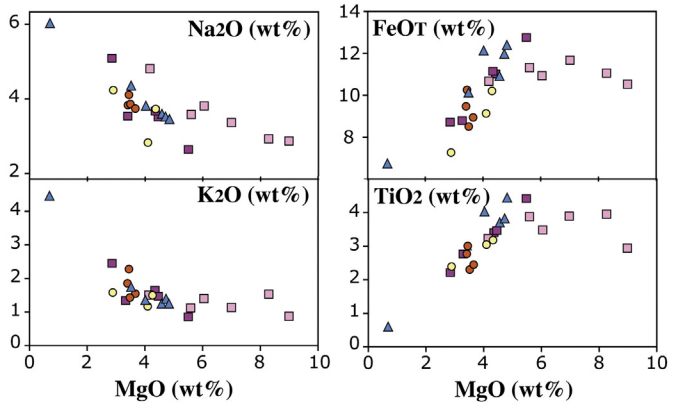

Fig. 3. Harker-like diagrams showing the compositional variations of our samples in Na_2O, K_2O, FeOT, and TiO_2 as a function of MgO (wt.%). Square symbols for S. Jorge, with dark and light color for samples older than 800 ka and younger than 750 ka, respectively; circles for Faial, with dark and light color for samples older than 800 ka and younger than 750 ka, respectively; triangles for Terceira.

Nevertheless, the Azores Archipelago lacks a clear age progression as observed on well-documented intra-plate linear chains of oceanic islands, e.g. in the Hawaiian-Emperor chain, or in French Polynesia (Bonneville et al., 2006; Hildenbrand et al., 2004). In contrast, recent unspiked K/Ar data and $^{40}Ar/^{39}Ar$ ages acquired on separated groundmass and pure mineral phases on samples from both S. Miguel (Johnson et al., 1998) and in the central Azores (e.g. Calvert et al., 2006; Hildenbrand et al., 2008, 2012; Larrea et al., 2014; Sibrant et al., 2014; and this study) reveal short episodes of coeval volcanic construction at the regional scale, e.g. around 850 ka, 700 ka, 400 ka, 200 ka, 120 ka, 50 ka, and during the historical period. Such synchronous volcanic construction cannot be explained simply as resulting from a stationary active mantle anomaly, unless we consider the pulsative and synchronous development of several small plumelets. It has been proposed recently that small P-wave velocity anomalies (Yang et al., 2006) could reflect density anomalies, which would trigger local convection in the form of narrow plumelets (Adam et al., 2013). However, it appears unrealistic that such inferred active features would promote short-lived (<50 kyr) events of partial melting at the same time under the various islands. Indeed, the development of small plumelets in the upper mantle, e.g., from a larger instability blocked at depth, typically occurs over timescales of several Myr to several tens of Myr, as evidenced in the region of the South Central Pacific in Polynesia (Bonneville et al., 2006; Courtillot et al., 2003; Davaille, 1999). Furthermore, the development of N150 and N110 volcanic ridges at the plateau scale is incompatible with present absolute plate movement towards SSW over stationary narrow plumelets (Hildenbrand et al., 2008).

We propose an alternative model that reconciles available geophysical, geochemical, geochronological and geological data. In this model, the enriched signatures expressed along the MAR and the several islands of the Azores, reflect the presence of residual enriched mantle zones dispersed in the shallow upper mantle (<300 km) under the Azores region. These could either represent the remnants of a large, presently dormant, heterogeneous mantle plume responsible for the formation of the Azores plateau several million years ago (Cannat et al., 1999; Silveira et al., 2006), and/or shallow delaminated lithospheric fragments inherited from the early stages of opening of the Atlantic (Moreira et al., 1999). Although recent trace element, Pb, Nd and Hf isotope data provide some evidence for the occurrence of lithospheric delamination, noble gas data from the Azores and adjacent MAR support the plume hypothesis with the entrainment of recycled oceanic lithosphere and surrounding upper mantle (Madureira et al., 2011). However, we argue that current deep mantle upwelling is not the main driving force responsible for the development of the recent volcanism. We propose instead that melt generation in the Central

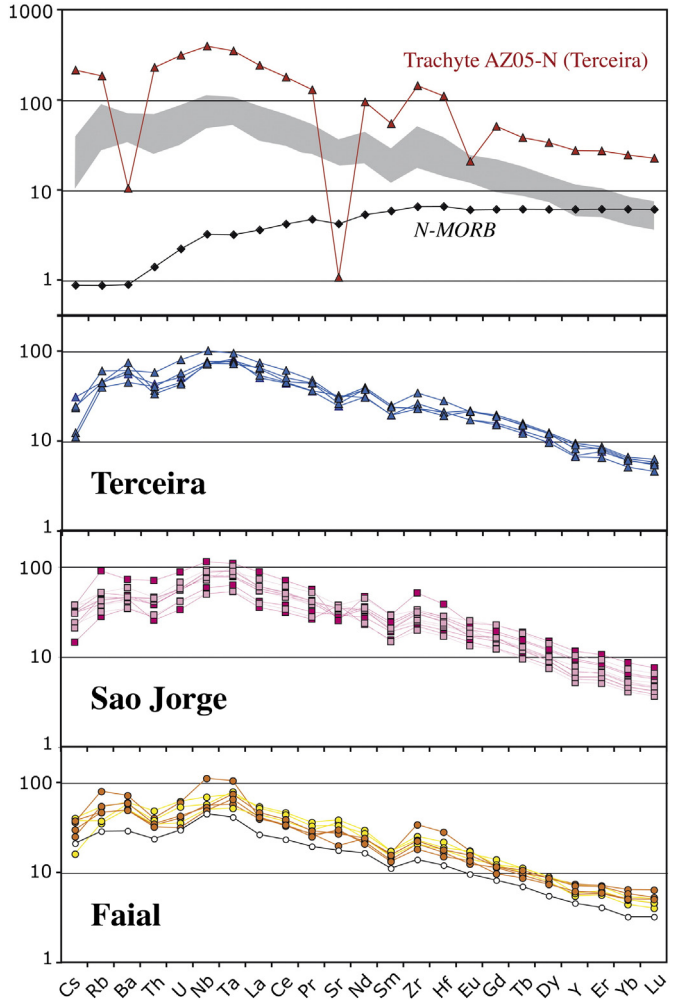

Fig. 4. Spiderdiagrams showing the distribution of trace elements for all our various samples (same symbols as in Fig. 3). The concentrations are normalized using the reference values given by McDonough and Sun (1995) for primitive mantle. Upper panel: the gry area shows the overall range of variations for the three islands (undistinguished), except for trachyte AZ05-N, which is shown separately (red curve). Lower 3 panels: spidergrams for each of the three islands—here studied. In the case of Faial, a primitive picrite (white circles, data from Beier et al., 2010) is shown for comparison.

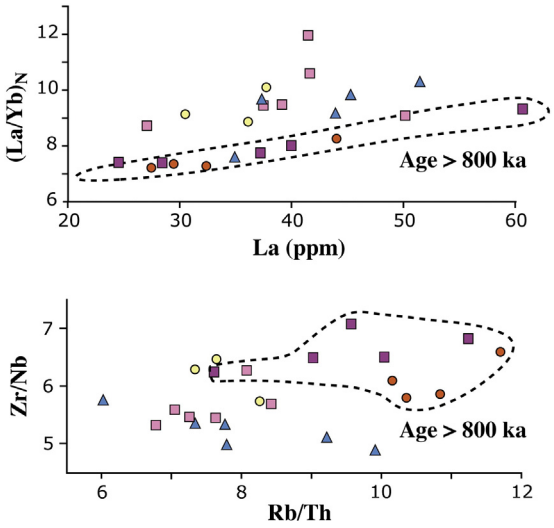

Fig. 5. Diagramms (La/Yb)N vs. La and (Zr/Nb) vs. (Rb/Th). The old lavas erupted on Faial and S. Jorge (age >800 ka) are distinguished. Same symbols as in Fig. 3.

Table 3
Isotopic composition of our samples from S. Jorge. Terceira and Faial. g: measurement on the groundmass separated for K/Ar dating (after Hildenbrand et al., 2008, 2012; Silva et al., 2012; and this study). Stars show the average composition after duplicate and replicate measurements for some of ours samples (full data shown in Supplementary material S3).

Sample	$^{87}Sr/^{86}Sr$	±(2SE)	$^{143}Nd/^{144}Nd$	±(2SE)	$^{208}Pb/^{204}Pb$	±(2SE)	$^{207}Pb/^{204}Pb$	±(2SE)	$^{206}Pb/^{204}Pb$	±(2SE)	$^{176}Hf/^{177}Hf$	±(2SE)
AZ05-C	0.703610	0.000009	0.512955	0.000006	39.3541	0.0020	15.6219	0.0008	20.0587	0.0009	0.283078	0.000006
AZ05-F	0.703588	0.000008	0.512963	0.000007	39.3348	0.0020	15.6172	0.0007	20.0206	0.0009	0.283066	0.000006
AZ05-G	0.703565	0.000008	0.512957	0.000006	39.2226	0.0022	15.6123	0.0007	19.9293	0.0008	0.283066	0.000004
AZ05-J	0.703556	0.000008	0.512968	0.000005	39.2621	0.0020	15.6166	0.0007	19.9960	0.0009	0.283073	0.000005
AZ05-K	0.703652	0.000008	0.512956	0.000005	39.2114	0.0025	15.6100	0.0010	19.8403	0.0009	0.283059	0.000005
AZ05-N	0.705523	0.000009	0.512960	0.000005	39.2486	0.0027	15.6091	0.0010	19.8677	0.0012	0.283068	0.000005
AZ05-P	0.703538	0.000009	0.513004	0.000006	38.9103	0.0028	15.5793	0.0010	19.7370	0.0012	0.283101*	0.000009*
AZ05-Pg	0.703517	0.000009	0.513003	0.000007	38.9250	0.0029	15.5848	0.0010	19.7453	0.0012	0.283094	0.000005
AZ05-R	0.703644	0.000009	0.512987	0.000008	38.8454	0.0019	15.5569	0.0006	19.5363	0.0008	0.283076	0.000005
AZ05-U	0.703627	0.000008	0.512977	0.000006	38.8144*	0.0045*	15.5479*	0.0028*	19.4757*	0.0029*	0.283061	0.000003
AZ05-Z	0.703608	0.000007	0.512967	0.000016*	38.9145	0.0018	15.5569	0.0006	19.5365	0.0007	0.283055	0.000004
AZ05-AB	0.703788	0.000007	0.512960	0.000006	38.7487	0.0025	15.5417	0.0009	19.3468	0.0007	0.283045	0.000005
AZ05-ABg	0.703778	0.000008	0.512958	0.000007	38.7440*	0.0012*	15.5397*	0.0020*	19.3486*	0.0039*	0.283037	0.000004
AZ05-AD	0.703746	0.000007	0.512964	0.000006	39.0641	0.0023	15.6244	0.0008	19.8015	0.0010	0.283058	0.000005
AZ05-ADg					39.0866	0.0026	15.6308	0.0008	19.8153	0.0013		
AZ05-AF	0.703643*	0.000006*	0.512984*	0.000007*	39.2752*	0.0020*	15.6289*	0.0006*	20.0923*	0.0017*	0.283080*	0.000014*
AZ05-AG	0.703705	0.000007	0.512987	0.000006	39.1046	0.0019	15.6199	0.0009	19.9007	0.0007	0.283080*	0.000021*
AZ05-AH	0.703787	0.000008	0.512891	0.000006	39.3232*	0.0043*	15.6310*	0.0056*	19.4947*	0.0018*	0.282966	0.000004
AZ05-AHg	0.703794	0.000007	0.512883*	0.000012*	39.3270*	0.0033*	15.6301*	0.0007*	19.4968*	0.0016*	0.282963	0.000005
AZ05-AJ	0.703569	0.000008	0.512941	0.000005	39.3827	0.0027	15.6212	0.0010	20.0234	0.0011	0.283039	0.000004
AZ05-AJg					39.3888*	0.0080*	15.6241*	0.0006*	20.0263*	0.0002*		
AZ05-ALg	0.703728	0.000008	0.512934	0.000006	39.0294*	0.0077*	15.5932*	0.0026*	19.6558*	0.0014*	0.282994	0.000005
AZ05-AM	0.703735	0.000007	0.512928	0.000006	39.0091*	0.0012*	15.5872*	0.0016*	19.6477*	0.0025*	0.282998	0.000005
AZ05-AMg	0.703750	0.000009	0.512936	0.000007	38.9961*	0.0058*	15.5818*	0.0005*	19.6417*	0.0023*	0.282999	0.000005
AZ05-AN	0.703874	0.000008	0.512898	0.000006	38.8634*	0.0058*	15.6192*	0.0029*	19.0905*	0.0047*	0.283000	0.000005
AZ05-ANg	0.703905	0.000008	0.512905	0.000006	38.8614*	0.0034*	15.6197*	0.0004*	19.0851*	0.0018*	0.283000	0.000006
AZ05-AO	0.703833	0.000009	0.512894	0.000006	39.2600*	0.0057*	15.6390*	0.0044*	19.5222*	0.0004	0.282986	0.000004
AZ05-AOg	0.703836	0.000008	0.512888	0.000007	39.2626*	0.0033*	15.6399*	0.0019*	19.5237*	0.0044*	0.282987	0.000005
AZ05-APg	0.703850	0.000009	0.512919	0.000007	38.8969	0.0024	15.6219	0.0009	19.1756	0.0010	0.283016	0.000005
AZ05-AQg	0.703796	0.000007	0.512908	0.000007	38.8247	0.0031	15.5593	0.0011	19.3622	0.0015	0.282965*	0.000010*
AZ05-AR	0.703737	0.000009	0.512929	0.000007	38.8396	0.0022	15.5568	0.0009	19.3262	0.0010	0.282995	0.000006
AZ05-ARg	0.703766	0.000007	0.512926	0.000006	38.8427	0.0025	15.5582	0.0009	19.3269	0.0011	0.282998	0.000004
BCR2	0.705004	0.000008	0.512645	0.000006	38.8343*	0.0027	15.6261*	0.0011	18.8042*	0.0012	0.282866	0.000005
BHVO-2	0.703466	0.000007	0.512986	0.000006	38.1929*	*0.0296*	15.4815*	*0.0069*	18.6354*	*0.0102*	0.283098	0.000005

Azores over the last 1.3 Myr has been mostly controlled by lithospheric deformation. A similar process has been pointed out on S. Miguel, where strong isotopic differences between lavas erupted synchronously by adjacent volcanoes suggest that the tectonic structure of the lithosphere locally controls mantle upwelling and partial melting (Haase and Beier, 2003). In the Central Azores, the two successive generations of volcanic ridges reported here suggest a rapid change of regional stresses between 850 and 750 ka. We propose that such re-organization reflects a major change in regional deformation accompanying the recent evolution of the Azores Triple Junction. In this interpretation, significant stretching of the lithosphere at the plateau scale first yielded the creation of new N150 oblique lithospheric structures in the whole area between the EAFZ and the present TR, prior to 800 ka (Fig. 10, stage 1). This likely caused significant decompression partial melting of the ambient upper mantle at a relatively high-degree, leading to a dilute expression of the enriched components, and yielding the production of melts with rather homogeneous trace element and isotopic composition relatively similar to lavas erupted synchronously at the MAR. Unfortunately, the use of classical thermo-barometers (e.g., Lee et al., 2009) is not possible for the vast majority of our samples, as most of them have a rather evolved composition. All our old samples from both S. Jorge and Faial, especially, have MgO < 6 wt.%. Fractionation may thus have significantly modified the initial composition of the primary magma, precluding any robust estimation of the ambient temperature and pressure during partial melting. However, the most primitive of the old samples (AZ05-P, MgO = 5.49 wt.%) has Tb/Yb and La/Yb ratios of 11.31 and 0.52, respectively, which support relatively deep melting of a mantle source within the garnet stability zone, and a degree of partial melting comprised between 5% and 8% (see Fig. 11 in Métrich et al., 2014). Considering the higher incompatible behavior of La during crystal fractionation in basaltic liquids, the initial La/Yb in the parental magma must have been significantly lower, and the actual degree of partial melting is probably closer to 8%.

The widespread development of N110 volcanic ridges during the last 750 kyr marks a major geodynamic reconfiguration (Fig. 10, stage 2), which can coincide in time with the individualization of the western part of the TR (Vogt and Jung, 2004). We note that the TR orientation to the west of Terceira, and the main strike of the several horsts and grabens presently active in the vicinity of S. Jorge and Pico–Faial volcanic ridges (Marques et al., 2013, 2014), are roughly paralell to Fracture Zones cutting the MAR between latitudes 38°N and 40°N. Accordingly, we interpret that the sudden re-organization of the Eurasia–Nubia plate boundary involved reactivation of preexisting lithospheric structures. The significant enrichment in LILE (including LREE), the higher $(La/Yb)_N$ ratios and the variable but general more radiogenic isotopic compositions in the young lavas (<750 kyr) support variable but overall lower degree of partial melting of the inferred fertile mantle sources. Such hypothesis is consistent with the recent work by Métrich et al. (2014), which showed that recent melt generation under Pico can be explained by decompression melting of a water-enriched mantle domain. For the sake of comparison, the Tb/Yb and La/Yb values for our sample AZ05-AD (age of 736 ± 12 ka, MgO = 8.9 wt.%) support relatively low degrees of partial meting (4–5%), in full agreement with what has been proposed in other recent studies conducted on young volcanics from the central Azores (e.g., Métrich et al., 2014; Zanon et al., 2013). Therefore, episodic magma production in the central Azores during the last 750 kyr can be explained by limited decompression melting associated with sporadic reactivation of inherited N110 transform faults, e.g. promoted by far-field stresses or MAR ridge-push.

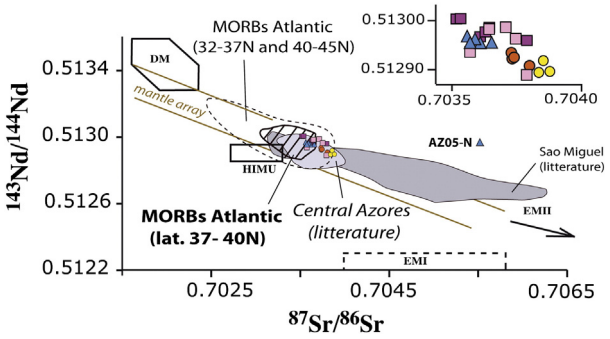

Fig. 6. Diagramm $^{143}Nd/^{144}Nd$ vs. $^{87}Sr/^{86}Sr$ showing the position of our samples from the three islands (same symbols as in Fig. 3), along with previous data acquired on MORBs and in the Azores (full data source in the text). The DM, HIMU, EMI and EMII mantle components are drawn after Zindler and Hart (1986). Upper inset: zoom showing the limited range of variation of our samples.

4.3. Implications for plate re-organization near triple junctions (TJs)

Among the 16 distinct types of TJs theoretically possible, only the ridge–ridge–ridge (R-R-R) type appears stable over a few million years (e.g. Georgen and Lin, 2002; McKenzie and Morgan, 1969).

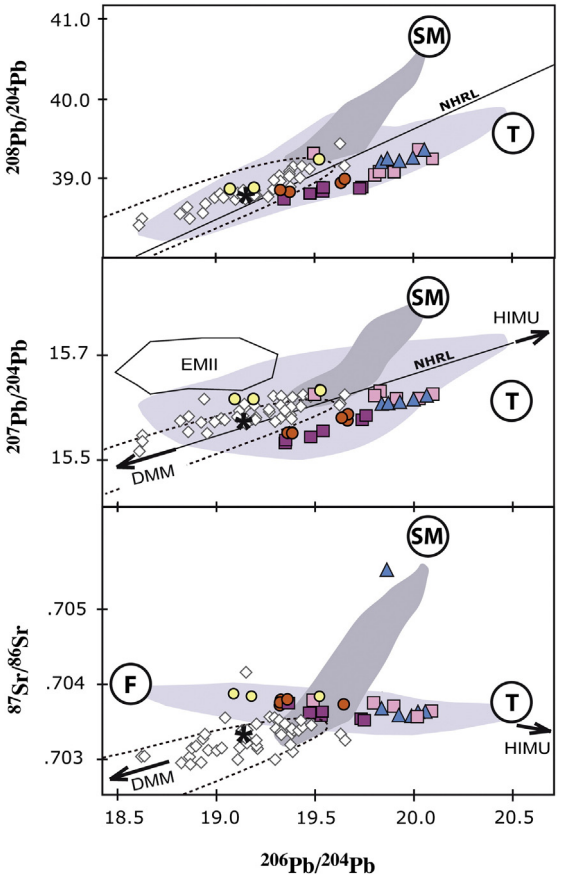

Fig. 7. Variations in $^{208}Pb/^{204}Pb$, $^{207}Pb/^{204}Pb$ and $^{87}Sr/^{86}Sr$ with respect to $^{206}Pb/^{204}Pb$ for our samples (same symbols as in Fig. 3). Diamonds show the composition of local MORBs dredged between latitudes 37 N and 40 N, whereas the star provides the corresponding average composition (data from Agranier et al., 2005; Dosso et al., 1999). The thin dashed line shows the compositional field of other MORBS dredged along the MAR outside the Azores area. The light gray and dark gray fields show the range of variation previously measured on samples from the central Azores and S. Miguel, respectively. Bold circles show local components, such as distinguished in previous studies (Millet et al., 2009; Moreira et al., 1999): SM: S. Miguel component; T: Topo end-member (S. Jorge); F: Faial end-member. NHRL: Northern Hemisphere Reference Line.

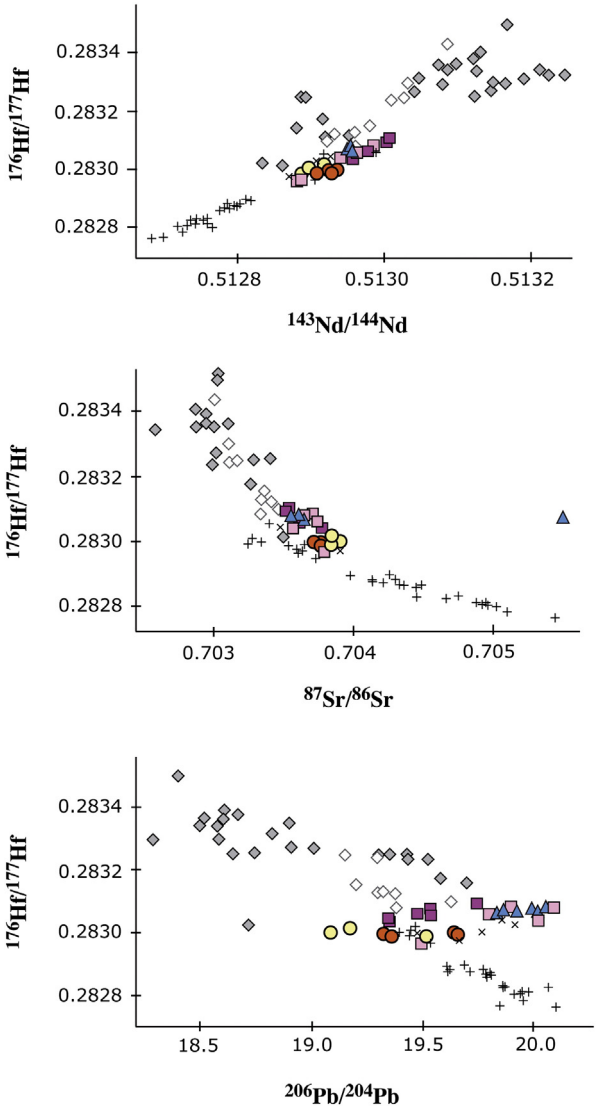

Fig. 8. Variations in $^{176}Hf/^{177}Hf$ with respect to $^{87}Sr/^{86}Sr$, $^{143}Nd/^{144}Nd$, and $^{206}Pb/^{204}Pb$ for our samples (same symbols as in Fig. 6). Dark diamonds for MAR samples between latitudes 33° and 37°N. Previous data on Pico (diagonal crosses) and S. Miguel (straight crosses) from Snyder et al. (2004) and Elliott et al. (2007).

The other types experience significant geometric re-organization through time, i.e. at least one of the branches may jump to reach a more stable configuration. The Azores Triple Junction (ATJ) appears to be a conspicuous illustration, as the eastern branch evolved from a mainly transform behavior (RRF-type TJ) towards a rift-type (RRR-type TJ). We note that the Terceira Rift (TR) and the northern part of the Azores plateau are presently the locus of significant oblique extension, as shown by the relationship between the TR orientation and plate velocities (e.g. DeMets et al., 2010) and focal mechanisms associated with recent medium/high magnitude earthquakes (e.g. Borges et al., 2007). Therefore, the TR may not represent the final stage of plate-reconfiguration, as proposed by Vogt and Jung (2004). The absence of well-defined magnetic anomalies on the seafloor remains a main limitation, as it either suggests that no significant oceanic accretion is occurring along the TR, or that oceanic accretion started too recently and at a too low spreading rate to generate detectable anomalies.

The present study provides significant new insights on the possible short-term behavior of plate re-configuration near such TJs. Our new data show that the eastern branch of the ATJ, at least during recent times, has not experienced a continuous shift towards the N. In contrast, the widespread development of oblique lithospheric structures inferred

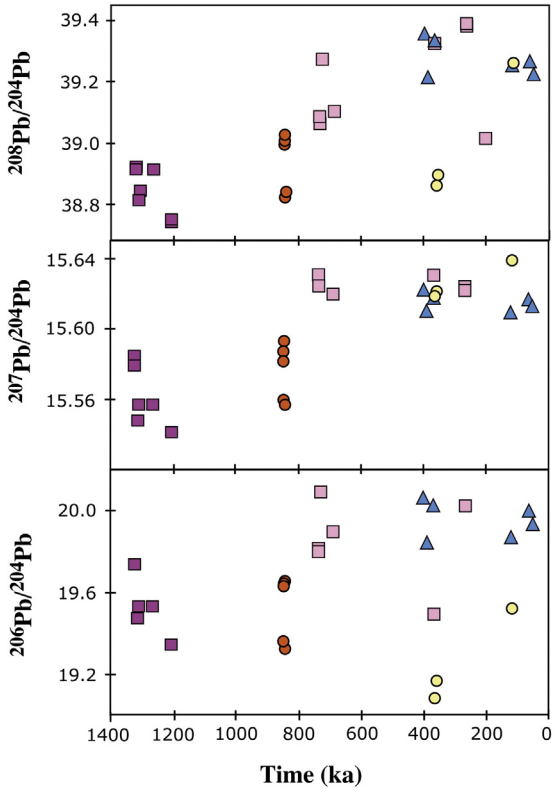

Fig. 9. Variations in $^{207}Pb/^{204}Pb$ through time. Same symbols as in Fig. 3.

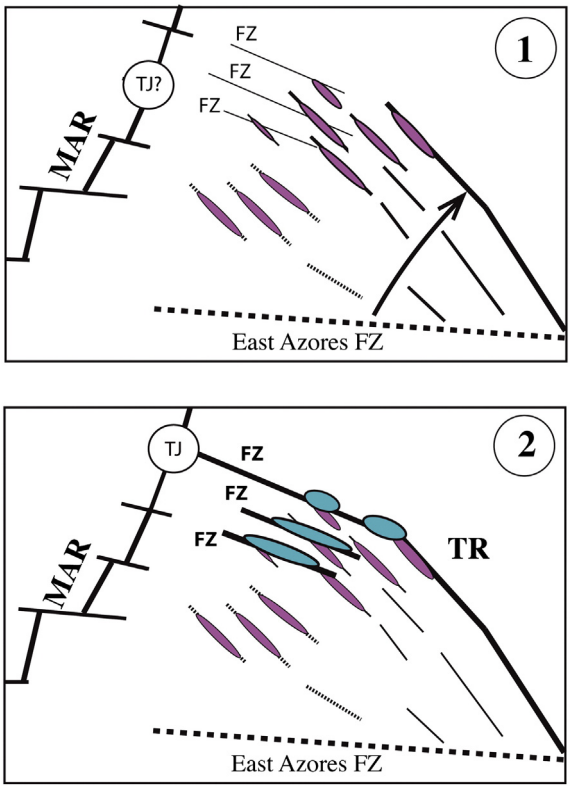

Fig. 10. Two-stage conceptual model depicting how the Eurasia–Nubia boundary reorganized from our new data: (1) diffuse stretching at the whole plateau scale yields the widespread creation of N150 oblique ridges prior to 850 ka; (2) at about 750 ka, sudden re-organization, with subsequent melt production/extraction controlled by re-activation of N110 FZ.

here suggests that large-scale diffuse intra-plate deformation may occur for a significant period (several Myr?) prior to sudden plate boundary jump. We are fully aware that the old volcanic successions on S. Jorge and Faial may have only recorded the latest history preceding ATJ reconfiguration, as numerous other oblique volcanic ridges over the Azores plateau (especially N of the East Azores Fracture Zone) remain to be investigated. We cannot exclude, for instance, that large-scale intra-plate deformation and oblique volcanic ridge development occurred in a diachronic way, e.g. from S to N, as suggested by a recent study (Sibrant et al., 2013). However, our data in the central Azores document large changes in melt generation and magma extraction around 800–750 ka, which suggests that such plate reconfiguration can effectively occur within only a few tens of thousands of years. The main question is whether such short period is sufficient to yield the creation/reactivation of N110 lithospheric structures and trigger significant changes in melt generation and extraction in a setting like the ATJ. Rubin and Macdougall (1988) constrained the combined duration of melting and magma transport to less than a few hundred thousand years. They concluded that ^{226}Ra excesses constrain the length of the magma transfer times from the melting depth through eruption to less than about a thousand years. Peate and Hawkesworth (2005) showed that the timescales of magmatic processes are comparable to the half-lives of several U series nuclides: 76 kyr for ^{230}Th, 33 kyr for ^{231}Pa, and 1.6 kyr for ^{226}Ra. This means that mantle melting and magma extraction to the surface should take a few tens to a couple of hundreds of kyr, depending on a number of regional factors, such as magma composition and viscosity, lithospheric thickness, tectonic setting, and regional stresses. The studied magmas in the central Azores are mostly low-viscosity basalts, and, according to Métrich et al. (2014), some of them particularly rich in water and volatiles. Although short-term magma ponding under the oceanic lithosphere and/or in short-lived crustal magma reservoir have episodically occurred (Zanon and Frezzotti, 2013; Zanon et al., 2013), the melts in the Azores thus can form and be extracted rapidly.

If most of the oceanic lithosphere is characterized by a brittle behavior, the relevant equation for fracture nucleation is Mohr–Coulomb's equation, which is independent of time or strain rate: $\tau = \sigma \tan(\phi) + C$, where τ is the shear strength, σ is the normal stress, C is the intercept of the failure envelope with the ordinate axis and is often called the cohesion, and ϕ is the angle of internal friction. This means that brittle rock yields by fracture when the differential stress reaches the brittle strength. However, in order for faults to grow to lithospheric scale, time is needed. If many faults form simultaneously, then a significant amount of time is needed, in the order of a few Myr (e.g. Cowie et al., 2000), to reach lithospheric scale dimension. However, master faults in the region under consideration are few. For instance, each side of the active TR is typically bounded by one or at most two master faults (Searle, 1980). Given the opening rate of the TR (ca. 2.4 mm/year according to Marques et al., 2013, 2014), its average depth (ca. 2000 m), and the average dip of normal faults (ca. 60°), then the vertical displacement rate is ca. 2 mm/year and the time needed to reach the TR's current depth is ca. 1 Ma. The oldest phase of sub-aerial volcanic construction within the TR has been constrained in S. Miguel at about 0.88 Ma (Johnson et al., 1998). There, the maximum time needed to bring melts to the surface through a new fault system (of lithospheric scale, and under a new stress field) is thus in the order of a hundred of kyr. The lithosphere under the central Azores is less than 20 Ma in age and is relatively thinner than under S. Miguel (e.g. Beier et al., 2008; Luís et al., 1994). In such conditions, the time necessary to produce significant changes in partial melting and magma extraction in the central Azores should not exceed a few tens of kyr. It may even be significantly less, as reactivation of pre-existing lithospheric structures is expected to occur faster than the creation of a new set of lithospheric faults. Therefore, it seems reasonable to infer that the several volcanic pulses here reported for the last 750 kyr result from successive brief (<50 kyr) episodes of melt generation and extraction to the surface. As the three islands here studied closely follow the present area of diffuse deformation (Marques et al., 2013, 2014), it also seems reasonable to infer

that the current diffuse plate boundary near the ATJ has been settled around 800–750 ka ago. Our study shows that inherited lithospheric structures such as fracture zones constitute preferential discontinuities for plate boundary re-localization near such TJs.

5. Conclusions

The combined geochronological and geochemical study presented here brings new constraints regarding source heterogeneity and melt production in the central Azores throughout the last 1.3 Myr. The distinction of two periods of volcanism older than 800 ka and younger than 750 ka especially provides an important basis for reinterpreting the compositional variability previously reported in the absence of a reliable temporal framework, and to discuss the main geodynamic processes that may have governed melt production and extraction over time.

The lavas analyzed range in composition from alkaline basalts/basanites to trachytes, and overall exhibit a strong enrichment in highly incompatible elements. The whole range of isotopic compositions we measured suggests the involvement of three components: (1) a weakly radiogenic component reflecting the source of regional MORBs, (2) a main HIMU-type component represented in the three islands, and (3) an additional component in Faial younger lavas, which appears similar to the EM type end-member previously recognized in other Azores eruptive complexes. The geographical distribution of the enriched components and the synchronous construction of various islands at the regional scale rules out an origin from a single narrow active plume. They suggest in turn the presence of dispersed residual enriched mantle domains, resulting from earlier fertilization of the upper mantle, possibly by the main plume event responsible for the formation of the Azores plateau several million years ago. The lavas erupted in S. Jorge and Faial prior to 800 ka have very homogeneous isotopic ratios, which partly overlap the compositional field of MORBs from the adjacent portion of the Mid-Atlantic Ridge (MAR). Their genesis can be explained by the regional development of N150 transtensive tectonic structures, which promoted significant decompression melting of the upper mantle, with correlative dilute expression of the enriched components. In contrast, the younger lavas (<750 ka) erupted along the N110 main structural direction on the three islands are significantly enriched in LILE, and generally have variable but more radiogenic isotopic compositions. Such characteristics suggest a lower-degree of partial melting and greater incorporation of fertile residual mantle portions during passive tectonic reactivation of pre-existing transform faults. We propose that the sub-aerial volcanism over the last 1.3 Myr in the central Azores record a sudden change in the conditions of melt generation, which most probably reveals a major reconfiguration of regional deformation accompanying the recent geodynamic reorganization of the Eurasia–Nubia plate boundary.

Supplementary data to this article can be found online at http://dx.doi.org/10.1016/j.lithos.2014.09.009.

Acknowledgments

We acknowledge P. Layer and an anonymous reviewer for their valuable comments, which helped to significantly improve the manuscript. Thanks to J. Barling, E. Barnes, M. Carpentier, Y. Feng, R. Friedman, B. Kieffer, M. Kuga, V. Lai, I. Nobre Silva, A. Shiel and J. Scoates for their help and fruitful discussions at PCIGR. This study was partially supported by French CNRS (Délégation Ile de France Sud, DR4), and by TEAMINT (POCTI/CTE/48137/2002) and EVOLV (PTDC/CTE-GIN/71838/2006) programs funded by FCT (Portugal). This is LGMT contribution 120.

References

Adam, C., Madureira, P., Miranda, J.M., Lourenço, N., Yoshida, M., Fitzenz, D., 2013. Mantle dynamics and characteristics of the Azores plateau. Earth and Planetary Science Letters 362, 258–271.

Agranier, A., Blichert-Toft, J., Graham, D., Debaille, V., Schiano, P., Albarède, F., 2005. The spectra of isotopic heterogeneities along the Mid-Atlantic Ridge. Earth and Planetary Science Letters 238, 96–109.

Asimow, P.D., Dixon, J.E., Langmuir, C.H., 2004. A hydrous melting and fractionation model for mid-ocean ridge basalts: application to the Mid-Atlantic Ridge near the Azores. Geochemistry, Geophysics, Geosystems 5 (1), 1–24.

Beier, C., 2006. The magmatic evolution of oceanic plateaus: a case study from the Azores(Ph.D. thesis) University of Kiel, Germany.

Beier, C., Haase, K.M., Abouchami, W., Krienitz, M.-S., Hauff, F., 2008. Magma genesis by rifting of oceanic lithosphere above anomalous mantle: Terceira Rift, Azores. Geochemistry, Geophysics, Geosystems 9, Q12013.

Beier, C., Turner, S., Plank, White, W., 2010. A preliminary assessment of the symmetry of source composition and melting dynamics across the Azores plume. Geochemistry, Geophysics, Geosystems 11, Q02004.

Beier, C., Haase, K.M., Turner, S.P., 2012. Conditions of melting beneath the Azores. Lithos 144–145, 1–11.

Bonatti, E., 1990. Not so "Hot Spots" in the oceanic mantle. Science 250, 107–110.

Bonneville, A., Dosso, L., Hildenbrand, A., 2006. Temporal evolution of the south-Pacific superplume activity: new data from the Cook-Australes volcanic chain. Earth and Planetary Science Letters 244 (1–2), 251–269.

Borges, J.F., Bezzeghoud, M., Buforn, E., Pro, C., Fitas, A., 2007. The 1980, 1997 and 1998 Azores earthquakes and some seismo-tectonic implications. Tectonophysics 435, 37–54.

Bourdon, B., Turner, S.P., Ribe, N.M., 2005. Partial melting and upwelling rates beneath the Azores from a U-series isotope perspective. Earth and Planetary Science Letters 239 (1–2), 42–56.

Calvert, A.T., Moore, R.B., McGeehin, J.P., Rodrigues da Silva, A.M., 2006. Volcanic history and 40Ar/39Ar and 14C geochronology of Terceira Island, Azores, Portugal. Journal of Volcanology and Geothermal Research 156 (1–2), 103–115.

Cannat, M., Briais, A., Deplus, C., Escartin, J., Georgen, J., Lin, J., Mercouriev, S., Meyzen, C., Muller, M., Pouliquen, G., Rabain, A., da Silva, P., 1999. Mid-Atlantic Ridge-Azores hotspot interactions: along-axis migration of a hotspot-derived event of enhanced magmatism 10 to 4 Ma ago. Earth and Planetary Science Letters 173 (3), 257–269.

Carpentier, M., Weis, D., Chauvel, C., 2013. Large U loss during weathering of upper continental crust: the sedimentary record. Chemical Geology 340, 91–104.

Chauvel, C., Hofmann, A.W., Vidal, P., 1992. HIMU-EM: the French Polynesian connection. Earth and Planetary Science Letters 110, 99–119.

Courtillot, V., Davaille, A., Besse, J., Stock, J., 2003. Three distinct types of hotspots in the Earth's mantle. Earth and Planetary Science Letters 205, 295–308.

Cowie, P.A., Gupta, S., Dawers, N.H., 2000. Implications of fault array evolution for synrift depocentre development: insights from a numerical fault growth model. Basin Research 12, 241–261.

Davaille, A., 1999. Simultaneous generation of hotspots and superswells by convection in a heterogenous planetary mantle. Nature 402, 756–760.

Davies, G.R., Norry, M.J., Gerlach, D.C., Cliff, R.A., 1989. A combined chemical and Pb-Sr-Nd isotope study of the Azores and Cape Verde hot-spots: the geodynamic implications. In: Saunders, A.D., N., M.J. (Eds.), Magmatism in the ocean basins. Geological Society Special Publication 42, pp. 231–235.

Debaille, V., Blichert-Toft, J., Agranier, A., Doucelance, R., Schiano, P., Albarede, F., 2006. Geochemical component relationships in MORB from the Mid-Atlantic Ridge, 22–35° N. Earth and Planetary Science Letters 241, 844–862.

DeMets, C., Gordon, R.G., Argus, D.F., 2010. Geologically current plate motions. Geophysical Journal International 181, 1–80.

Dosso, L., Bougault, H., Langmuir, C., Bollinger, C., Bonnier, O., Etoubleau, J., 1999. The age and distribution of mantle heterogeneity along the Mid-Atlantic Ridge (31–41 degrees N). Earth and Planetary Science Letters 170, 269–286.

Dupré, B., Lambret, B., Allègre, C.J., 1982. Isotopic variations within a single volcanic island - the Terceira case. Nature 299, 620–622.

Elliott, T., Blichert-Toft, J., Heumann, A., Koetsier, G., Forjaz, V., 2007. The origin of enriched mantle beneath Sao Miguel, Azores. Geochimica et Cosmochimica Acta 71, 219–240.

Flower, M.F.J., Schmincke, H.-U., Bowman, H., 1976. Rare earth and other trace elements in historic Azorean lavas. Journal of Volcanology and Geothermal Research 1, 127–147.

Gente, P., Dyment, J., Maia, M., Goslin, J., 2003. Interaction between the Mid-Atlantic Ridge and the Azores hotspot during the last 85 Myr: emplacement and rifting of the hotspot-derived plateaus. Geochemistry, Geophysics, Geosystems 4, 8514.

Georgen, J.E., Lin, J., 2002. Three-dimensional passive flow and temperature beneath ocean ridge–ridge–ridge triple junctions. Earth and Planetary Science Letters 204, 115–132.

Georgen, J.E., Sankar, R.D., 2010. Effects of ridge geometry on mantle dynamics in an oceanic triple junction region: implications for the Azores Plateau. Earth and Planetary Science Letters 298, 23–34.

Gillot, P.Y., Hildenbrand, A., Lefèvre, J.C., Albore-Livadie, C., 2006. The K/Ar dating method: principle, analytical techniques and application to Holocene volcanic eruptions in southern Italy. Acta Vulcanologica 18 (1–2), 55–66.

Gurenko, A.A., Hoernle, K.A., Hauff, F., Schmincke, H.-U., Han, D., Miura, Y.N., Kaneoka, I., 2006. Major, trace element, and Nd-Sr-Pb, O-He-Ar isotope signatures of shield stage lavas from the central and western Canary Islands. Chemical Geology 233, 75–112.

Haase, K.M., Beier, C., 2003. Tectonic control of ocean island basalt sources on São Miguel, Azores? Geophysical Research Letters 30 (16), 1856.

Halliday, A.N., Davies, G.R., Lee, D.-C., Tommasini, S., Paslick, C.R., Fitton, J.G., James, D.E., 1992. Lead isotope evidence for young trace element enrichment in the oceanic upper mantle. Nature 359, 623–627.

Hanano, D., Scoates, J.S., Weis, D., 2009. Alteration mineralogy and the effect of acid-leaching on the Pb-isotope systematics of ocean-island basalts. American Mineralogist 94, 17–26.

Hart, S.R., 1984. A large-scale isotope anomaly in the southern hemisphere mantle. Nature 309, 753–757.
Hildenbrand, A., Gillot, P.-Y., Le Roy, I., 2004. Volcano-tectonic and geochemical evolution of an oceanic intra-plate volcano: Tahiti-Nui (French Polynesia). Earth and Planetary Science Letters 217 (3), 349–365.
Hildenbrand, A., Madureira, P., Ornelas Marques, F., Cruz, I., Henry, B., Silva, P., 2008. Multi-stage evolution of a sub-aerial volcanic ridge over the last 1.3 Myr: S. Jorge Island, Azores Triple Junction. Earth and Planetary Science Letters 273, 289–298.
Hildenbrand, A., Marques, F.O., Costa, A.C.G., Sibrant, A.L.R., Silva, P.M.F., Henry, B., Miranda, J. M., Madureira, P., 2012. Reconstructing the architectural evolution of volcanic islands from combined K/Ar, morphologic, tectonic, and magnetic data: the Faial Island example (Azores). Journal of Volcanology and Geothermal Research 241–242, 39–48.
Hildenbrand, A., Marques, F.O., Costa, A.C.G., Sibrant, A., Silva, P., Henry, B., Miranda, M., Madureira, P., 2013. Reply to the comment by Quartau and Mitchell on "Reconstructing the architectural evolution of volcanic islands from combined K/Ar, morphologic, tectonic, and magnetic data: The Faial Island example (Azores)", J. Volcanol. Geotherm. Res. 241–242, 39–48, by Hildenbrand et al. (2012). Journal of Volcanology and Geothermal Research 255, 127–130.
Hofmann, A.W., 2003. Sampling mantle heterogeneity through oceanic basalts: isotopes and trace elements. In: Carlson, R.W. (Ed.), The Mantle and Core 2In: Holland, H., Turekian, K.K. (Eds.), Treatise on Geochemistry. Elsevier- Pergamon, Oxford, pp. 61–101.
Holm, P.M., Wilson, J.R., Christensen, B.P., Hansen, L., Hansen, S.L., Hein, K.M., Mortensen, A.K., Pedersen, R., Plesner, S., Runge, M.K., 2006. Sampling the Cape Verde mantle plume: evolution of melt compositions on Santo Antao, Cape Verde Islands. Journal of Petrology 47 (1), 145–189.
Jackson, M.G., Dasgupta, R., 2008. Compositions of HIMU, EM1, and EM2 from Global Trends between Radiogenic Isotopes and Major Elements in Ocean Island Basalts. Earth and Planetary Science Letters 276, 175–186.
Jean-Baptiste, P., Allard, P., Coutinho, R., Ferreira, T., Fourré, E., Queiroz, G., Gaspar, J.L., 2009. Helium isotopes in hydrothermal volcanic fluids of the Azores archipelago. Earth and Planetary Science Letters 281, 70–80.
Johnson, C.L., Wijbrans, J.R., Constable, C.G., Gee, J., Staudigel, H., Tauxe, L., Forjaz, V.H., Salgueiro, M., 1998. Ar-40/Ar-39 ages and paleomagnetism of Sao Miguel lavas, Azores. Earth and Planetary Science Letters 160, 637–649.
Larrea, P., Wijbrans, J.R., Gale, C., Ubide, T., Lago, M., Franca, Z., Widom, E., 2014. Ar-40/Ar-39 constraints on the temporal evolution of Graciosa Island, Azores (Portugal). Bulletin of Volcanology 76 (2), 796. http://dx.doi.org/10.1007/s00445-014-0796-8.
Lee, C.T.A., Luffi, P., Plank, T., Dalton, H., Leeman, W.P., 2009. Constraints on the depths and temperatures of basaltic magma generation on Earth and other terrestrial planets using new thermobarometers for mafic magmas. Earth and Planetary Science Letters 279, 20–33.
Lourenço, N., Miranda, J.M., Luis, J.F., Ribeiro, A., Victor, L.A.M., Madeira, J., Needham, H.D., 1998. Morpho-tectonic analysis of the Azores Volcanic Plateau from a new bathymetric compilation of the area. Marine Geophysical Research 20 (3), 141–156.
Luís, J.F., Miranda, J.M., Galdeano, A., Patriat, P., Rossignol, J.C., Mendes Victor, L.A., 1994. The Azores Triple Junction evolution since 10 Ma from an aeromagnetic survey of the Mid-Atlantic Ridge. Earth and Planetary Science Letters 125, 439–459.
Madureira, P., Moreira, M., Mata, J., Allègre, C.J., 2005. Primitive neon isotopes in Terceira Island (Azores archipelago). Earth and Planetary Science Letters 233 (3–4), 429–440.
Madureira, P., Mata, J., Mattielli, N., Queiroz, G., Silva, P., 2011. Mantle source heterogeneity, magma generation and magmatic evolution at Terceira Island (Azores archipelago): constraints from elemental and isotopic (Sr, Nd, Hf, and Pb) data. Lithos 126, 402–418.
Marques, F.O., Catalão, J.C., DeMets, C., Costa, A.C.G., Hildenbrand, A., 2013. GPS and tectonic evidence for a diffuse plate boundary at the Azores Triple Junction. Earth and Planetary Science Letters 381, 177–187.
Marques, F.O., Catalão, J.C., DeMets, C., Costa, A.C.G., Hildenbrand, A., 2014. Corrigendum to "GPS and tectonic evidence for a diffuse plate boundary at the Azores Triple Junction" [Earth Planet. Sci. Lett. 381 (2013) 177–187]. Earth and Planetary Science Letters 387, 1–3.
McDonough, W.F., Chauvel, C., 1991. Sample contamination explains the Pb isotopic composition of some Rurutu island and Sasha seamount basalts. Earth and Planetary Science Letters 105, 397–404.
McDonough, W.F., Sun, S.-S., 1995. The composition of the Earth. Chemical Geology 120, 223–253.
McKenzie, D.P., Morgan, W.J., 1969. Evolution of triple junctions. Nature 224, 125–133.
Métrich, N., Zanon, V., Créon, L., Hildenbrand, A., Moreira, M., Marques, F.O., 2014. Is the "Azores hotspot" a wetspot? Insights from geochemistry of fluid and melt inclusions in olivine of Pico basalt. Journal of Petrology 55, 377–393.
Millet, M.-A., Doucelance, R., Baker, J.A., Schiano, P., 2009. Reconsidering the isotopic variations in ocean isalnd basalts : insights from a fine-scale study of São Jorge Island, Azores archipelago. Chemical Geology 265, 289–302.
Montelli, R., Nolet, G., Dahlen, F.A., Masters, G., Engdahl, R.E., Hung, S.H., 2004. Finite-frequency tomography reveals a variety of plumes in the mantle. Science 303, 338–343.
Montelli, R., Nolet, G., Dahlen, F.A., Masters, G., 2006. A catalogue of deep mantle plumes: new results from finite frequency tomography. Geochemistry, Geophysics, Geosystems 7, Q11007. http://dx.doi.org/10.1029/2006GC001248.
Moreira, M., Doucelance, R., Dupré, B., Kurz, M., Allègre, C.J., 1999. Helium and lead isotope geochemistry in the Azores archipelago. Earth and Planetary Science Letters 169, 189–205.
Moreira, M., Kanzari, A., Madureira, M., 2012. Helium and neon isotopes in São Miguel island basalts, Azores Archipelago: new constraints on the "low 3He" hotspot origin. Chemical Geology 322–323, 91–98.
Nobre Silva, I., Weis, D., Barling, J., Scoates, J.S., 2009. Basalt leaching systematics and consequences for Pb isotopic compositions by MC-ICP-MS. Geochemistry, Geophysics, Geosystems 10, Q08012. http://dx.doi.org/10.1029/2009GC002537.
Nobre Silva, I., Weis, D., Scoates, J.S., 2010. Effects of acid leaching on the Sr-Nd-Hf isotopic compositions of ocean island basalts. Geochemistry, Geophysics, Geosystems 11, Q09011. http://dx.doi.org/10.1029/2010GC003176.
Nobre Silva, I., Weis, D., Scoates, J.S., 2013. Isotopic systematics of the early Mauna Kea shield phase and insight into the deep mantle beneath the Pacific Ocean. Geochemistry, Geophysics, Geosystems 14 (3). http://dx.doi.org/10.1002/ggge.20047.
Oversby, V.M., 1971. Lead in oceanic islands : Faial, Azores and Trindade. Earth and Planetary Science Letters 11, 401–406.
Peate, D.W., Hawkesworth, C.J., 2005. U series disequilibria: insights into mantle melting and the timescales of magma differentiation. Reviews of Geophysics 43, RG1003. http://dx.doi.org/10.1029/2004RG000154.
Pilidou, S., Priestley, K., Debayle, E., Gudmundsson, O., 2005. Rayleigh wave tomography in the North Atlantic: high resolution images of the Iceland, Azores and Eifel mantle plumes. Lithos 79, 453–474.
Pretorius, W., Weis, D., Williams, G., Hanano, D., Kieffer, B., Scoates, J.S., 2006. Complete trace elemental characterization of granitoid (USGS G-2, GSP-2) reference materials by high resolution inductively coupled plasma-mass spectrometry. Geostandards and Geoanalytical Research 30, 39–54.
Rubin, K.H., Macdougall, J.D., 1988. ^{226}Ra excesses in mid-ocean-ridge basalts and mantle melting. Nature 335, 158–161.
Schilling, J.G., 1975. Azores mantle blob: rare earth evidence. Earth and Planetary Science Letters 25, 103–115.
Searle, R., 1980. Tectonic pattern of the Azores spreading centre and triple junction. Earth and Planetary Science Letters 51, 415–434.
Sibrant, A.L.R., Hildenbrand, A., Marques, F.O., Costa, A.C.G., 2013. Volcano-tectonic evolution of Santa Maria Island: implications for the Nubia-Eurasia plate boundary in the Azores. Fall Meeting, San Francisco, USA.
Sibrant, A.L.R., Marques, F.O., Hildenbrand, A., 2014. Construction and destruction of a volcanic island developed inside an oceanic rift: Graciosa Island, Terceira Rift, Azores. Journal of Volcanology and Geothermal Research 284, 32–45.
Silva, P.F., Henry, B., Marques, F.O., Hildenbrand, A., Madureira, P., Mériaux, C.A., Kratinová, Z., 2012. Palaeomagnetic study of a sub-aerial volcanic ridge (São Jorge Island, Azores) for the past 1.3 Myr: evidence for the Cobb Mountain Subchron, volcano flank instability and tectono-magmatic implications. Geophysical Journal International 188 (3), 959–978.
Silveira, G., Stutzmann, E., Davaille, A., Montagner, J.-P., Mendes-Victor, L., Sebai, A., 2006. Azores hotspot signature in the upper mantle. Journal of Volcanology and Geothermal Research 156, 23–34.
Snyder, D.C., Widom, E., Pietruszka, A.J., Carlson, R.W., 2004. The role of open system processes in the development of silicic magma chambers: a chemical and isotopic investigation of the Fogo A trachytic deposit, Sao Miguel, Azores. Journal of Petrology 45, 723–738.
Sridhar, D.I., Ray, D., 2003. Structure, tectonic and petrology of mid-oceanic ridges and the Indian scenario. Current Science 85 (3), 277–289.
Steiger, R.H., Jäger, E., 1977. Subcommission on geochronology: convention on the use of decay constants in geo and cosmochronology. Earth and Planetary Science Letters 36, 359–362.
Turner, S., Hawkesworth, C., Rogers, N., King, P., 1997. U-Th isotope disequilibria and ocean island basalt generation in the Azores. Chemical Geology 139 (1–4), 145–164.
Vogt, P.R., Jung, W.Y., 2004. The Terceira Rift as hyper-slow, hotspot-dominated oblique spreading axis: a comparison with other slow-spreading plate boundaries. Earth and Planetary Science Letters 218, 77–90.
Weis, D., Frey, F.A., 1991. Isotope geochemistry of the Ninetyeast Ridge basement basalts: Sr, Nd, and Pb evidence for involvement of the Kerguelen hot spot. Proceeding of the Ocean Drilling Program, Scientific Results 121, 591–610.
Weis, D., Frey, F.A., 1996. Role of the Kerguelen plume in generating the eastern Indian Ocean seafloor. Journal of Geophysical Research 101, 13,381–13,849.
Weis, D., Kieffer, B., Maerschalk, C., Pretorius, W., Barling, J., 2005. High-precision Pb-Sr-Nd-Hf isotopic characterization of USGS BHVO-1 and BHVO-2 reference materials. Geochemistry, Geophysics, Geosystems 6, Q02002. http://dx.doi.org/10.1029/2004GC000852.
Weis, D., Kieffer, B., Maerschalk, C., Pretorius, W., Barling, J., 2006. High-precision Pb-Sr-Nd-Hf isotopic characterization of USGS BHVO-1 and BHVO-2 reference materials. Geochemistry, Geophysics, Geosystems 6 (2), 1–10. http://dx.doi.org/10.1029/2004GC000852.
Weis, D., et al., 2007. Hf isotope compositions of US Geological Survey reference materials. Geochemistry, Geophysics, Geosystems 8, Q06006. http://dx.doi.org/10.1029/2006GC001473.
White, W.M., Hofmann, A.W., 1982. Sr and Nd isotope geochemistry of oceanic basalts and mantle evolution. Nature 296, 821–825.
White, W.M., Schilling, J.-G., Hart, S.R., 1976. Evidence for the Azores mantle plume from strontium isotope geochemistry of the Central North Atlantic. Nature 263, 659–663.
White, W.M., Tapia, M.D.M., Schilling, J.-G., 1979. The petrology and geochemistry of the Azores Islands. Contributions to Mineralogy and Petrology 69, 201–213.
Widom, E., Carlson, R.W., Gill, J.B., Schmincke, H.-U., 1997. Th-Sr-Nd-Pb isotope and trace element evidence for the origin of the São Miguel, Azores, enriched mantle source. Chemical Geology 140, 49–68.
Wilson, M., 1989. Igneous petrogenesis. A global tectonic approach. Chapman and Hall, London (466 pp.).
Yang, T., Shen, Y., van der Lee, S., Solomon, S.C., Hung, S.H., 2006. Upper mantle structure beneath the Azores hotspot from finite-frequency seismic tomography. Earth and Planetary Science Letters 250 (1–2), 11–26.
Zanon, V., Frezzotti, M.L., 2013. Magma storage and ascent conditions beneath Pico and Faial islands (Azores archipelago): a study on fluid inclusions. Geochemistry, Geophysics, Geosystems 14 (9), 3494–3514.
Zanon, V., Kueppers, U., Pacheco, J.M., Cruz, I., 2013. Volcanism from fissure zones and the Caldeira central volcano of Faial Island, Azores archipelago: geochemical processes in multiple feeding systems. Geological Magazine 150 (3), 536–555.
Zindler, A., Hart, 1986. Chemical geodynamics. Annual Review of Earth and Planetary Sciences 14, 493–571.